Stable Mn^{2+}, Cu^{2+} and Ln^{3+} complexes with cyclen-based ligands functionalized with picolinate pendant arms[†]

Aurora Rodríguez-Rodríguez[a], Zoltán Garda[b], Erika Ruscsák[b], David Esteban-Gómez[a], Andrés de Blas[a], Teresa Rodríguez-Blas[a], Luís M. P. Lima[c], Maryline Beyler[c], Raphaël Tripier[c], Gyula Tircsó[b] and Carlos Platas-Iglesias[a]

[a] Departamento de Química Fundamental, Universidade da Coruña, Rúa da Fraga 10, A Coruña, Spain

[b] Department of Inorganic and Analytical Chemistry, Faculty of Science and Technology, University of Debrecen, Egyetem tér 1, H-4032 Debrecen, Hungary

[c] Université de Bretagne Occidentale, UMR-CNRS 6521, SFR ScInBioS, UFR des Sciences et Techniques, 6 avenue Victor le Gorgeu, 29238 Brest Cedex 3, France

How to cite:

Abstract

In this study we present the results of the equilibrium, dissociation kinetics, DFT and X-ray crystallographic studies performed on the complexes of metal ions of biomedical importance (Mn^{2+}, Cu^{2+} and Gd^{3+}) formed with octadentate ligands based on a cyclen platform incorporating two picolinate pendant arms ($dodpa^{2-}$ and $Medodpa^{2-}$). The stability constants of the complexes were accessed by multiple methods (pH-potentiometry, direct and competition UV-vis spectrophotometry and ^{1}H-relaxometry). The stability constants of the complexes formed with $dodpa^{2-}$ and $Medodpa^{2-}$ do not differ significantly (*e.g.* log $K_{[Mn(dodpa)]}$ = 17.40 *vs.* log $K_{[Mn(Medodpa)]}$ = 17.46, log $K_{[Cu(dodpa)]}$ = 24.34–25.17 *vs.* log $K_{[Cu(Medodpa)]}$ = 24.74 and log $K_{[Gd(dodpa)]}^{+}$ = 17.27 *vs.* log $K_{[Gd(Medodpa)]}^{+}$ = 17.59), which indicates that the steric hindrance brought by the methyl groups has no significant effect on the stability of the complexes. The stability constants of the Mn^{2+} complexes formed with the cyclen dipicolinates were found to be *ca.* 3 log K units higher than those determined for the complex of the cyclen monopicolinate ($dompa^{-}$), which indicates that the second picolinate moiety attached to the backbone of the macrocycle is very likely coordinated to the Mn^{2+} ion. However, the stability of the [Cu(dodpa)] and [Cu(Medodpa)] complexes agrees well with the stability constant of $[Cu(dompa)]^{+}$, in line with the hexadentate coordination around the metal ion observed in the X-ray structure of [Cu(Medodpa)]. The $[Gd(dodpa)]^{+}$ and $[Gd(Medodpa)]^{+}$ complexes display a fairly high kinetic inertness, as the rate constants of acid catalysed dissociation ($k_1 = 2.5(4) \times 10^{-3}$ and $8.3(4) \times 10^{-4}$ M^{-1} s^{-1} for $[Gd(dodpa)]^{+}$ and $[Gd(Medodpa)]^{+}$, respectively) are smaller than the value reported for [Gd(do3a)] ($k_1 = 2.5 \times 10^{-2}$ M^{-1} s^{-1}). The [Mn(dodpa)] complex was found to be more inert than [Mn(Medodpa)]. The results of the diffusion ordered NMR spectroscopy (DOSY) and DFT calculations of diamagnetic $[La(dodpa)]^{+}$ and $[Lu(dodpa)]^{+}$ complexes indicate the formation of a trinuclear entity of the La complex in aqueous solution.

Keywords: cyclen-based ligands; lanthanide complexes; crystal structures; transition-metal complexes; picolinate pendants
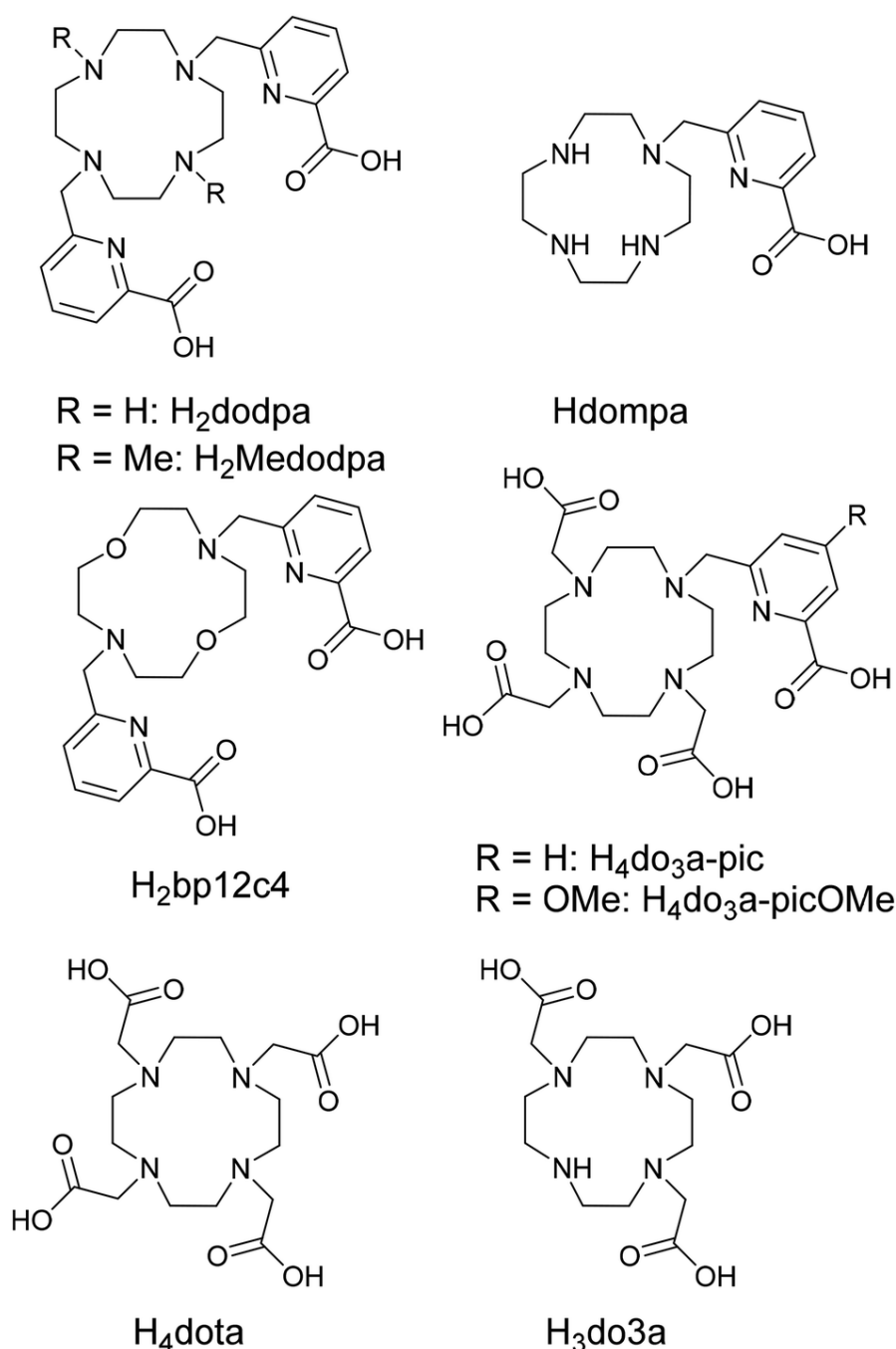
Introduction

Complexes formed with polyaza-polycarboxylate ligands and their derivatives containing amide, phosphinate, phosphonate or alcohol OH moieties have attracted considerable attention in recent years due to their successful application in medical diagnosis and therapy. Complexes of open-chain and macrocyclic polyamines are now routinely used as carriers of radionuclides in Positron Emission Tomography (PET), Single Photon Emission Computed Tomography (SPECT), or RadioImmunoTherapy (RIT).[1] Besides, complexes of paramagnetic metal ions such as Gd^{3+} are applied as contrast agents in Magnetic Resonance Imaging (MRI),[2] while compounds containing an appropriate antenna in order to sensitize Ln^{3+} luminescence have potential application in optical imaging.[3] However, research in this field appears to be shifting towards the use of macrocyclic chelators owing to the favourable coordinating properties of these types of ligands. Indeed, the complexes considered for *in vivo* use must fulfil well defined requirements; among these, fine-tuning of thermodynamics, kinetics (formation and dissociation) and redox stabilities through careful ligand design remains an important goal for coordination chemists. The complexes formed by macrocyclic ligands were often found to be very inert even in competitive biological media (containing proteins, bioligands, biogenic metal ions, *etc.*), but they are also known to form more slowly.[4] Thus, tailoring new ligands with improved complexation properties for various applications is still very challenging.

Designing ligands for biomedical applications requires the selection of ligand structures, allowing for a specific functionalization of the backbone (*i.e.* C- or N-functionalized ligands). This allows obtaining, for instance, more rigid (and more inert) complexes or producing bifunctional chelating agents (BCAs), which contain a chemically reactive group suitable for linking the complexes to their carriers, vectors, *etc.*[5] Another important point in the ligand design is the proper selection of the pendant arms to be used, as it may affect considerably the physicochemical properties of the complexes (stability, inertness, redox potential, *etc.*) or can act as a built-in chromophore capable of efficient Ln^{3+} sensitization.[6] In this respect, the pyridinecarboxylate (picolinate) moiety is a very versatile building block, as it has been shown to provide strong coordination toward different metal ions (Mn^{2+}, Cu^{2+} and Ln^{3+} ions) when attached to both linear and macrocyclic platforms.[7–10] Indeed, in the last ten years, ligands incorporating one, two or three pyridinecarboxylate units derived from open chain (iminodiacetic ($imda^{2-}$), nitrilotriacetic (nta^{3-}), ethylenediamine-tetraacetic ($edta^{4-}$) and *trans*-1,2-diaminocyclohexane-*N,N,N′,N′*-tetraacetic ($tcdta^{4-}$) acids), as well as macrocyclic polyamines (based on 1,4,7-triazacyclononane, 1,4,7,10-tetraazacyclododecane, 1,4,8,11-tetraazacyclotetradecane along with their cross-bridged derivatives) were prepared and their complexes characterized in solution and in the solid state.[7–9] As a result of the intense research on this topic, different ligands containing picolinate groups were shown to provide: (1) Ln^{3+} complexes endowed with remarkably high thermodynamic stability and satisfactorily high inertness,[11] (2) excellent selectivity for the lighter Ln^{3+} ions over the heavier ones (allowing us to develop separation procedures for lanthanide(III) and actinide(III) ions),[12] (3) efficient sensitization of Eu^{3+} and Tb^{3+} luminescence,[6,11] or (4) Gd^{3+} complexes with very high water exchange rates.[8,13] As mentioned before, certain applications require the attachment of a biomolecule (*e.g.* functionalization *via* the reactive group methodology) responsible for taxiing the chelates *in vivo* (BCAs). In this respect synthetic strategies showed that the 4-position of the pyridine ring of the picolinate moiety is easily accessible.[14]

In recent studies, we have reported a series of octadentate ligands based on 12-membered macrocycles containing one or two pyridinecarboxylate units ($do3a\text{-}pic^{4-}$, $do3a\text{-}picOMe^{4-}$, $bp12c4^{2-}$, $dodpa^{2-}$ and $Medodpa^{2-}$) designed for stable Ln^{3+} ion complexation in aqueous solution (Scheme 1).[9,11,15] The Ln^{3+} complexes of these ligands were characterized both in solution (^1H, ^{13}C, and ^{17}O NMR, DFT calculations, luminescence lifetime measurements) and in the solid state (X-ray crystallography). However data concerning the stability and inertness of their complexes are available only for some systems ($do3a\text{-}pic^{4-}$, $do3a\text{-}picOMe^{4-}$ and $bp12c4^{2-}$).[8,11] Thus, the aim of the work reported here was to investigate the thermodynamic stability and kinetic inertness of the complexes formed by $dodpa^{2-}$ and $Medodpa^{2-}$ with

some metal ions with potential biomedical interest (Mn^{2+}, Cu^{2+} and Gd^{3+}). Gd^{3+} and Cu^{2+} were chosen due to the importance of the complexes of these metal ions in MRI and PET imaging, respectively,[1,2] while Mn^{2+} was selected due to the increasing recent effort reported in the literature to develop Mn^{2+}-based MRI contrast agents.[16] The equilibrium processes in these systems were characterized by pH-potentiometry, UV-vis spectrophotometry and ^1H-relaxometry. The kinetic inertness of the Mn^{2+} and Gd^{3+} complexes was accessed by studying respectively the metal exchange reactions occurring between the Mn^{2+} complexes and the Cu^{2+} ion and the acid catalysed dissociation for the $[Gd(dodpa)]^+$ and $[Gd(Medodpa)]^+$ complexes. The structure of the $Medodpa^{2-}$ ligand and its monomeric Cu^{2+} complex was characterised by X-ray crystallography in the solid state, while diffusion-ordered spectroscopy (DOSY), Hartree–Fock (HF) and density functional theory (DFT) calculations were used to gain information about the unexpected self-aggregation of the $[La(Medodpa)]^+$ complex in aqueous solution.

R = H: H$_2$dodpa
R = Me: H$_2$Medodpa

Hdompa

H$_2$bp12c4

R = H: H$_4$do$_3$a-pic
R = OMe: H$_4$do$_3$a-picOMe

H$_4$dota

H$_3$do3a

Scheme 1. Ligands discussed in the present work.

Results and discussion

The protonation constants of dodpa^{2-} and Medodpa^{2-} were determined by pH-potentiometric titrations; the constants and standard deviations are given in Table 1, which also lists the protonation constants of related ligands. Ligand protonation constants were calculated from the overall equilibrium constants (log β_{01R} where $R = 1$ to 6), as defined in eqn (1) and (2):

$$PM + QL + RH \leftrightarrows M_P L_Q H_R \tag{1}$$

$$\beta_{PQR} = \frac{[M_P H_Q L_R]}{[M]^P [H]^R [L]^Q} \tag{2}$$

Thus, the protonation constants of the ligands and complexes were calculated using the following equations:

$$K_i^H = \frac{[H_i L]}{[H_{i-1} L][H^+]} \tag{3}$$

$$K_{MHiL} = \frac{[MH_i L]}{[MH_{i-1} L][H^+]} \tag{4}$$

The data shown in Table 1 indicate that the first protonation constants of dodpa^{2-} and Medodpa^{2-} are very similar, while the second protonation constant K^H_2 is *ca.* 1.2 units higher in dodpa^{2-}. This result suggests that HMedodpa$^-$ is stabilized by intramolecular hydrogen-bonding interactions. The first protonation constant is somewhat lower than that reported for do3a^{3-}and dota^{4-},[17] but similar to that determined for dompa$^-$,[18] which can be partially ascribed to the electron withdrawing effect of the picolinate pendant arm.[19] Different studies on 1,4,7,10-tetraazacyclododecane derivatives have revealed that the first two protonation processes occur on nitrogen atoms of the macrocycle situated in a *trans* position. As stated earlier,[8] the third and fourth protonation constants can be assigned to the picolinate moiety, while the fifth protonation process most likely occurs on a third nitrogen atom of the macrocycle. The first two protonation constants of dodpa^{2-} and Medodpa^{2-} are two log K units higher than those of the diaza-12-crown-4 derivative bp12c4^{2-}.

The X-ray crystal structure of the [H$_4$Medodpa]$^{2+}$ cation confirms the proposed protonation constant assignments (Fig. 1). Indeed, the two *trans* N atoms of the cyclen unit containing methyl substituents and the carboxylate groups of the ligand are protonated. In addition, the protonated N atoms are involved in hydrogen-bonding interactions with the N atoms of the pyridyl groups. The 12-membered macrocycle adopts a square [3333] conformation similar to that observed for protonated forms of dota^{4-} and related ligands,[20] in which the ligand is predisposed to bind metal ions.

Table 1. Protonation and stability constants characterizing the equilibrium involving the dodpa^{2-} and Medodpa^{2-} ligands as well as their Mn^{2+}, Cu^{2+} and Gd^{3+} complexes (25 °C).

	dodpa[a] 0.15 M NaCl	Medodpa[a] 0.15 M NaCl	do3a[a] 0.15 M NaCl	do3a[g] 0.1 M KCl	dota[g] 0.1 M KCl	dompa[h] 0.15 M NaCl	bp12c4[i] 0.1 M KCl
Log K^H_1	11.16(1)	11.36(1)	10.07(5)	11.99	11.41	11.22	9.16
Log K^H_2	10.11(1)	8.88(3)	8.93(6)	9.51	9.83	9.38	7.54
Log K^H_3	4.06(2)	4.12(4)	4.43(9)	4.30	4.38	3.39	3.76
Log K^H_4	3.50(3)	3.50(3)	4.11(7)	3.63	4.63		2.79
Log K^H_5	0.90(2)	1.18(2)	1.88(7)	1.84	1.92		
Σlog K^H_4	28.83	27.86	27.54	29.43	30.25		23.25
Log β_{MnL}	17.33(1)[b]	17.42(1)[b]	16.76(2)		19.89	14.48	
	17.75(3)[c]	17.73(2)[c]					
Log β_{MnHL}	21.20(4)	20.74(1)	20.70(2)		24.15	18.51	
Log β_{MnH2L}			23.88(3)		27.14		
Log β_{CuL}	24.34(5)[d]	24.74(2)[f]		25.75	22.25	24.0	19.56
	24.44(3)[e]					25.06[e]	
	25.17(4)[f]						
Log β_{CuHL}	29.63(5)[c]	30.18(2)[f]		29.4	26.03	25.83	26.08
	29.74(3)[e]					26.92[e]	
	29.61(2)[f]						
Log K_{CuHL}	5.27(4)[d]	5.58(8)[d]					
	5.29(5)[e]	5.38(6)[d]					
	5.30(3)[f]	5.44(9)[f]					
Log β_{CuH2L}	31.49(5)[b]			31.09	29.08		
	31.64(3)[d]						
	31.62(2)[e]						
Log K_{CuH2L}	1.91(4)[b]						
	2.01(3)[d]						
	1.88(2)[e]						
Log β_{GdL}	17.27(16)[c]	17.59(12)[c]		21.56	24.0		18.82
				21.1[g]			
Log β_{GdHL}				23.16[g]	26.30		

a This work. *b* Obtained from potentiometric titrations. *c* Obtained from relaxometric data. *d*Obtained with UV-vis measurements. *e* Obtained by simultaneous analysis of UV-vis and potentiometric data. *f* Combined pH-potentiometric and UV-vis competition methods by using bimp^{5-} (edta^{4-} in the case of [Cu(dompa)]$^+$). *g* Taken from ref. 17; a log K^H_6 value was also reported for dota^{4-}. *h* Taken from ref. 18. *i* Taken from ref. 8.

The thermodynamic stability of the Mn^{2+} complexes of dodpa^{2-} and Medodpa^{2-} were obtained using potentiometric pH titrations with 1 : 1 Mn^{2+} : ligand ratios. During the titrations a brown precipitate (presumably MnO(OH)$_2$) was formed at high pH values (pH = 11–12), and therefore this pH range was not used for stability constant determination. The titration curves (Fig. S1 and S2, ESI†) could be fitted assuming the formation of both protonated ([MnH(L)]$^+$) and di-protonated ([MnH$_2$(L)]$^{2+}$) complex species. However, good agreement between the species distribution curve obtained by pH-potentiometry and the ^{1}H-relaxometric profile obtained as a function of pH could only be achieved when only monoprotonated species were considered (Fig. S3, ESI†). The stability constants determined for the dodpa^{2-} and

Medodpa^{2-} complexes are very similar, indicating that the presence of methyl groups in the latter does not introduce significant steric hindrance for the coordination of the ligand to the metal ion (Table 1). The species distribution diagrams (Fig. S4, ESI†) indicate that the dissociation of the complexes starts below pH~5.0, and consequently the formation of the protonated form [MnH(L)]$^{+}$ (L = dodpa^{2-} or Medodpa^{2-}) is observed in the pH range of 3.0–5.0.

Stability constant determination was also performed using ^{1}H relaxometry, as the determination of stability constants using independent methods provides more reliable results. The relaxivities of [Mn(dodpa)] and [Mn(Medodpa)] at neutral pH (25 °C, 20 MHz) are 1.02 and 1.04 mM^{-1} s^{-1}, respectively. These values are close to those observed for Mn^{2+} complexes that lack inner-sphere water molecules such as [Mn(do3a)]$^{-}$.[21] The relaxivity of both complexes steadily increases below pH ~ 5, reaching a value of 8.16 mM^{-1} s^{-1} at pH < 3. This relaxivity value corresponds to that of [Mn(H$_2$O)$_6$]$^{2+}$,[22] which confirms that the increase in proton relaxivity observed below pH 5 is due to the dissociation of the complex. The stability constants obtained from potentiometric and relaxometric pH titrations are in excellent agreement (Table 1), although it must be stressed out that the stability constant of the protonated complex could not be determined reliably using the relaxometric method. This can be explained in terms of small differences in the relaxivities of the [Mn(dodpa)] and [Mn(Hdodpa)]$^{+}$ complexes, as well as the relatively low abundance of the protonated species (max. ~35% at pH = 3.80; Fig. S3, ESI†).
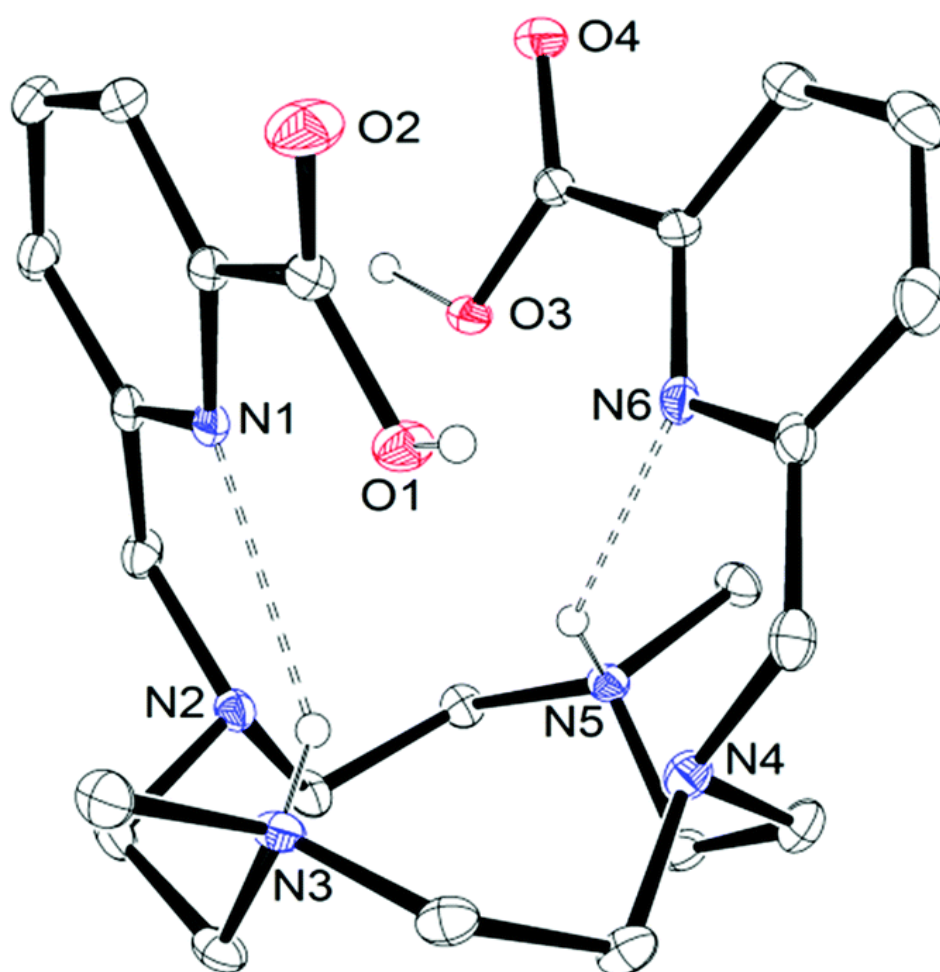

Fig. 1. View of the structure of the [H$_4$Medodpa]$^{2+}$ cation present in crystals of Na[H$_4$Medodpa](CF$_3$COO)$_3$·CF$_3$COOH (hydrogen-bonding data: N(3)···N(1), 3.100(3) Å, N(3)–H(3)···N(1), 2.42 Å, N(3)–H(3)···N(1), 144.7°; N(5)···N(6), 3.050(3) Å, N(5)–H(5)···N(6), 2.31 Å, N(5)–H(5)···N(6), 139.8°).

A comparison of the stability constants determined for the Mn^{2+} complexes of dodpa^{2-} and Medodpa^{2-} with those determined for the [Mn(dompa)]$^+$ complex indicates that the attachment of a second picolinate moiety to the macrocyclic polyamine backbone results in a noticeable increase in the stability of their Mn^{2+} complexes. Indeed, the log K_{MnL} values determined for the complexes of dodpa^{2-} and Medodpa^{2-} are *ca.* 3 log K units higher than those determined for [Mn(dompa)]$^+$. This is confirmed by the calculation of pMn values, defined as pMn = −log[Mn]$_{free}$, for pH = 7.4, c_L = 10 μM and c_{Mn}^{2+} = 1 μM.[23]Indeed, the protonation constants and stability constants listed in Table 1 provide the following pMn values: 11.81 (dodpa^{2-}), 12.92 (Medodpa^{2-}) and 9.07 (dompa$^−$).[18] These results suggest that the second picolinate unit of dodpa^{2-} and Medodpa^{2-} is involved in coordination to the Mn^{2+} ion, thereby contributing to the enhancement of the stability of these complexes.

The Cu^{2+} complexes of dodpa^{2-} and Medodpa^{2-} were titrated using pH-potentiometry. However, the fitting of the titration curves indicated that the complexes (monoprotonated and diprotonated complexes) were formed quantitatively already at acidic pH (pH ∼ 1.8). Thus, only protonation equilibria of the complexes in the pH range 1.8–11.8 could be determined from these data. However, it became clear that either a direct spectrophotometric measurement with the use of the d–d absorption band of the complexes or a competition titration with an appropriate open-chain ligand (*e.g.* edta^{4-}) followed by UV-vis spectrophotometry, combined with pH-potentiometry, must be used to determine the stability of these complexes.[18] At first, out-of-cell samples were prepared and equilibrated in strongly acidic media for a week (H$^+$ ion concentration was in the range of 15.91–714.8 mM for the dodpa^{2-} and 15.86–631.5 mM for the Medodpa^{2-} systems). Subsequently, the visible absorption spectra were acquired (Fig. 2, S6 and S7, ESI†), and the molar absorption coefficients of the [Cu(L)] and [Cu(HL)] complexes of dodpa^{2-} and Medodpa^{2-} were determined at 11 wavelengths near the absorption maxima (550–800 nm). A simultaneous fitting of pH-potentiometric and UV-vis titration data acquired in the pH range of 1.85–8.26 was performed (at two different total concentrations), which provided the equilibrium constants characterizing the Cu^{2+} : dodpa^{2-} : H$^+$ system. Unfortunately, in the case of the Medodpa^{2-} system some precipitation occurred in the samples with high acid concentrations. Therefore, a ligand-competition method was applied for stability constant determination in which the Cu^{2+} : dodpa^{2-}-H$^+$ system was used as a test system, since in this case it was possible to determine reliable stability constants by direct methods. The bimp^{5-} ligand (H$_5$bimp = bis(iminodicarboxymethyl-*N*-methyl)phosphinic acid; Fig. S5, ESI†) was selected as a competing chelator, as the stabilities of its Cu^{2+} complexes were determined by multiple methods [log $K_{[Cu(bimp)]}^{2-}$ = 19.3 by pH-potentiometry (I = 1.0 M Me$_4$NCl) and log $K_{[Cu(bimp)]}^{2-}$ = 17.5 and log $K_{[Cu2(bimp)2]}^{4-}$ = 40.0 for the dimer by 2D EPR spectroscopy (I = 0.10 M NaCl)].[24] The corresponding log $K_{[Cu(bimp)]}^{2-}$ value obtained in the current study by using a combined pH-potentiometric and UV-vis spectrophotometric approach equals 18.34(3) (I = 0.15 M NaCl), which is in acceptable agreement with the previously reported data. Using the protonation constants of dodpa^{2-} and bimp^{5-} ligands and the stability constants of the Cu^{2+} complexes formed with these ligands, a speciation distribution curve was calculated in order to estimate the pH range where the competition titration can be carried out (Fig. 3).

The curves shown in Fig. 3 indicate that the competition reaction may be carried out either in the pH range of 3.6–4.0 where competition occurs between [Cu(Hdodpa)]$^+$ and [Cu(bimp)]$^{3-}$ complexes or above pH = 7.0, where the exchange between [Cu(dodpa)] and [Cu(bimp)]$^{3-}$ complexes may serve as a tool for stability constant determination. Both pH ranges were tested, but at high pH the Cu^{2+} exchange between the ligands was found to occur slowly at room temperature. Therefore, samples containing 1.99 mM Cu^{2+} and 2.042 mM dodpa^{2-} with increasing amounts of the bimp^{5-} ligand (concentration range 2.052–50.05 mM) in the pH range 3.76–4.10 were prepared, equilibrated for 24 hours and their spectra were recorded (Fig. S8, ESI†). Being in possession of the molar absorption coefficients of absorbing species present in the equilibrium, the stability constants of the [Cu(Hdodpa)]$^+$ and [Cu(dodpa)] complexes were determined (Table 1; the fitting parameter was 0.0040 absorbance units for the 164 data points fitted). As can be seen from the data listed in Table 1, excellent agreement was found for the cumulative constant characterizing the formation of the

[Cu(Hdodpa)]$^+$ complex determined by other techniques and using the above described competition method. The stability constant of the [Cu(dodpa)] complex turned out to deviate slightly from that determined by the simultaneous fitting of the pH-potentiometric and UV-vis spectroscopic data, which is not very surprising since the fraction of the given complex present in the equilibrium in the pH range used for the studies remains always below 20%. However, using the equilibrium constant determined for [Cu(Hdodpa)]$^+$ = [Cu(dodpa)] + H$^+$ from independent studies (pH-potentiometric and UV-vis methods) it is possible to calculate log $K_{[Cu(dodpa)]}$. Applying the same method to the Cu^{2+} : Medodpa^{2-} : H$^+$ system for the samples containing 1.99 mM Cu^{2+} and 2.019 mM Medodpa^{2-} with increasing amounts of the bimp^{5-} ligand (concentration range 2.002–80.28 mM, pH range 3.63–4.30, Fig. S9, ESI†) allowed us to estimate the cumulative constant characterizing the formation of the [Cu(HMedodpa)]$^+$ complex (Table 1). As for [Cu(dodpa)], the stability constant of [Cu(Medodpa)] was calculated with the use of its deprotonation constant.
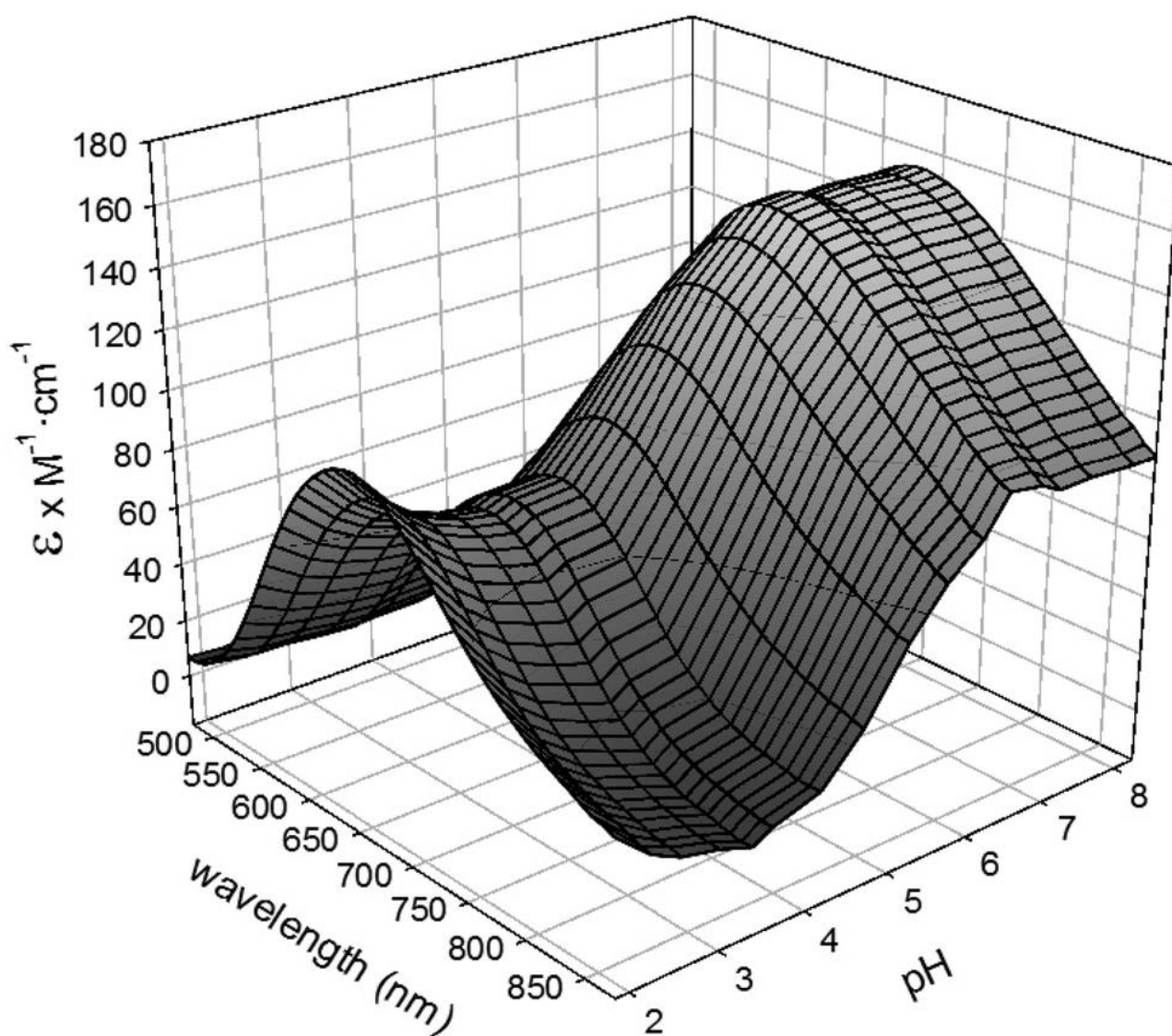

Fig. 2. Absorption spectra of the Cu^{2+}–dodpa^{2-} system as a function of −log c_{H}^+ recorded in the range of −log c_{H}^+ = 1.81–8.15 (I = 0.15 M NaCl; [Cu^{2+}] = [dodpa] = 1.654 mM, l = 1 cm, 25 °C).

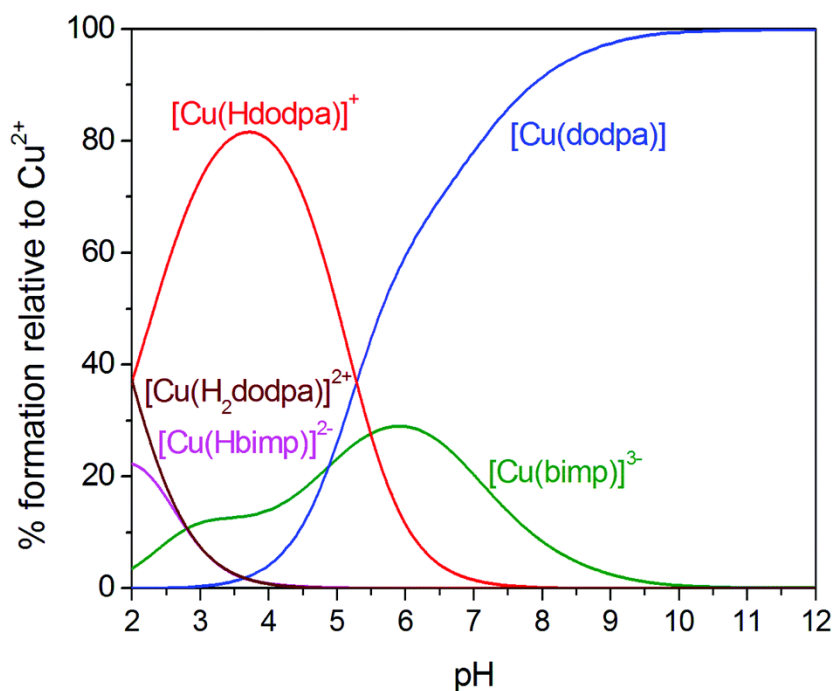**Fig. 3.** Species distribution diagram for the Cu^{2+}:dodpa : bimp system (1 : 1 : 1) ([Cu^{2+}] = [dodpa] = [bimp] = 2×10^{-3} M).

Owing to the slow rates of complexation often observed for reactions of Ln^{3+} ions and macrocyclic ligands, stability constant determination was attempted by equilibrating solutions containing stoichiometric amounts of the Ln^{3+} ion (Gd^{3+} or Ce^{3+}) and the ligand (dodpa^{2-} or Medodpa^{2-}) at pH values for which complexation is expected to take place (pH = 5.45). The rate of complex formation was assessed by following the changes in the UV-Vis absorption spectrum (Ce^{3+}) or relaxivity (Gd^{3+}) of the solution during the course of several months (Fig. S10, ESI†). These preliminary studies showed that the thermodynamic equilibrium was not reached even after six months. To circumvent this problem, the stability of the Gd^{3+} complexes was assessed by provoking the partial dissociation of the complexes upon decreasing the pH. For that purpose, the [Gd(dodpa)]$^+$ and [Gd(Medodpa)]$^+$ complexes were prepared using strong heating at high pH values (8.6 and 9.8, respectively, see the Experimental section for full details) by gradual NaOH additions. Batch solutions of the complexes (1 mM) covering the pH range 2.5–8.0 with the use of a buffer cocktail consisting of piperazine (pip), N-methyl-piperazine (nmp) and N,N′-dimethyl-piperazine (dmp) were prepared, and the dissociation of the complexes was followed using the relaxometric method. Solutions of the complexes at three representative pH values were taken (3.00, 4.94 and 7.05) to assess the time required to reach thermodynamic equilibrium. The relaxivity of these solutions was followed over time, reaching the steady state after four months.

The relaxivity of equilibrated solutions of [Gd(dodpa)]$^+$ and [Gd(Medodpa)]$^+$ at different pH values was used to estimate the stability constants of these complexes. The relaxivity data show that complexation occurs in the pH range 2.5–5.0 (Fig. 4). The relaxivities of [Gd(dodpa)]$^+$ and [Gd(Medodpa)]$^+$ recorded above pH 5.5 (25 °C, 20 MHz) amount to 3.28 and 2.01 mM^{-1} s^{-1}, respectively. These values are in agreement with those reported previously,[15] while below pH 5.5 the relaxivity increases due to the dissociation of the complex. At pH 3.0 the observed relaxivity values correspond well to the value reported for [Gd(H$_2$O)$_8$]$^{3+}$.[25] The thermodynamic stabilities of [Gd(dodpa)]$^+$ and [Gd(Medodpa)]$^+$ (log $K_{[Gd(dodpa)]^+}$ = 17.27(16) and log $K_{[Gd(Medodpa)]^+}$ = 17.59(12)) are clearly lower than those of the complexes with dota^{4-} and do3a^{3-}, and one order of magnitude lower than those reported for the related ligand bp12c4^{2-}.
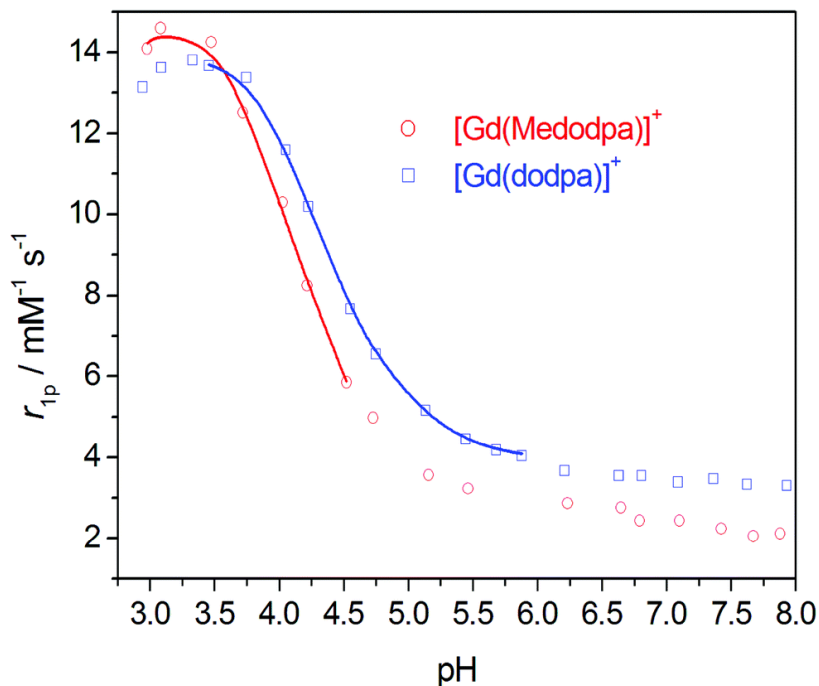
Fig. 4. Relaxivity pH profiles of the equilibrated [Gd(dodpa)]$^+$ and [Gd(Medodpa)]$^+$ complexes ([Gd(L)]$^+$ = 1.0 × 10^{-3} M in a buffer cocktail consisting of 25–25–25 mM of pip, nmp and dmp, t = 25 °C, I = 0.15 M NaCl, B = 0.47 T).

Acid catalysed dissociation of the Gd^{3+} complexes and metal exchange reactions of the Mn^{2+} complexes

The dissociation of Gd^{3+} and other metal complexes *in vivo* may proceed by different pathways:[26] (1) spontaneous dissociation, characterized by a rate constant k_0; (2) proton assisted dissociation characterized by the protonation constants K_{GdHL} and K_{GdH2L} and rate constants k_{GdHL} and k^H_{GdHL} (often denoted as k_1 and k_2); (3) ligand-assisted dissociation characterized by the stability constant of mixed ligand complexes K_{LGdL*} and rate constant k_{LGdL*}; (4) metal-ion-catalysed dissociation characterized by the stability constant of the dinuclear complexes K_{GdLM} (where M = Zn, Cu or Eu) and rate constant k_{GdLM} (often expressed as k^M_3). The dissociation of complexes with macrocyclic ligands such as dota^{4-} often occurs very slowly due to their compact and highly rigid structure, which results in high kinetic inertness towards complex dissociation. As a consequence, the acid catalysed process constitutes the main dissociation pathway for the complexes of this class, with the ligand assisted and metal-ion-catalysed pathways being negligible.[4,17]

The acid-catalysed dissociation rates of [Gd(dodpa)]$^+$ and [Gd(Medodpa)]$^+$ complexes have been studied using the relaxometric method. In the case of [Gd(dodpa)]$^+$, acid solutions with HCl concentrations in the range 0.01–0.25 M were used. However, the [Gd(Medodpa)]$^+$ complexes were found to be significantly more inert, and therefore higher acid concentrations had to be employed (0.01–0.8 M). Under these conditions the complexes are thermodynamically unstable and dissociate completely. The rates of dissociation can be expressed by eqn (5):

$$-\frac{d[ML]_t}{dt} = k_{obs}[ML]_t \tag{5}$$

Plots of the obtained k_{obs} values *vs.* H$^+$ concentration for the different complexes are shown in Fig. 5. These plots are characteristic of a quadratic dependence on proton concentration, which indicates that the dissociation might take place by both the proton-independent (characterized by k_0) and the proton-assisted pathways with the formation and dissociation of mono- and diprotonated complexes (characterized by k_1 and k_2, respectively). Similar quadratic dependencies were observed for the acid catalysed dissociation of [Ce(dota)]$^-$,[27] [Eu(do3a-pic)]$^-$ (ref. 11) and [Ce(bp12c4)]$^+$.[8] For other complexes with macrocyclic ligands such as [Eu(dota)]$^-$ and [Ln(pcta)] these plots show a saturation behaviour, which indicates that the complexes dissociate following the formation of a protonated complex species.[4,28] Thus, the observed first order dissociation rate constants were fitted to eqn (6):

$$k_{obs} = \frac{k_0 + k_H K_{[M(HL)]}[H^+] + k_H^H K_{[M(HL)]} K_{[M(H_2L)]}[H^+]^2}{1 + K_{[M(HL)]}[H^+] + K_{[M(HL)]} K_{[M(H_2L)]}[H^+]^2} \qquad (6)$$

Fits of the experimental data according to eqn (6) showed that for both complexes, $1 \gg K_{[Gd(HL)]}[H^+] + K_{[Gd(HL)]} K_{[Gd(H_2L)]}][H^+]^2$. Thus, eqn (6) can be simplified to give:

$$k_{obs} = k_0 + k_1[H^+] + k_2[H^+]^2 \qquad (7)$$

where k_0 is the rate constant characterizing the spontaneous dissociation process and k_1 and k_2 the rate constants associated with the proton assisted pathway. The results obtained from the fittings are summarized in Table 2. The dissociation of [Gd(dodpa)]$^+$ is characterized by a k_1 constant that is one order of magnitude lower than that of the do3a^{3-} complex, which shows that the [Gd(dodpa)]$^+$ complex is remarkably inert. The k_1 value determined for [Gd(Medodpa)]$^+$ is even smaller, which indicates that the introduction of the methyl groups into positions 1 and 7 of the cyclen unit results in a significant decrease of the rate constants characterizing the proton-assisted dissociation pathway. The k_1 values determined for [Gd(dodpa)]$^+$ and [Gd(Medodpa)]$^+$ fall between those reported for the complexes of do3a^{3-} and dota^{4-}. The analysis of the kinetic data for [Gd(Medodpa)]$^+$ indicates that spontaneous dissociation also contributes to the overall decomplexation process, most likely due to the slower proton assisted mechanism. Due to the different mechanisms operating for these systems, their kinetic inertness was assessed by calculating their k_{obs} values with [H$^+$] = 0.1 M. From these values the half-life of each complex under these conditions was obtained as $t_{1/2} = \ln 2/k_{obs}$. The $t_{1/2}$ values indicate the following sequence of kinetic inertness for this family of Gd^{3+} complexes: do3a^{3-} < dodpa^{2-} < Medodpa^{2-} < dota^{4-}. The higher kinetic inertness of [Gd(Medodpa)]$^+$ compared to [Gd(dodpa)]$^+$ is probably related to the more compact structure of the former, which is associated with the steric hindrance caused by the methyl groups and results in the absence of coordinated water molecule.[15] Interestingly, both [Gd(dodpa)]$^+$ and [Gd(Medodpa)]$^+$ are considerably more inert than the related complex [Gd(bp12c4)]$^+$, for which k_{obs} can be estimated to be 0.1 s^{-1} at [H]$^+$ = 0.1 M in the absence of exchanging metal ions, yielding a half-life of 6.9 s under these conditions. Furthermore, the dissociation rates of [Gd(bp12c4)]$^+$ were found to increase significantly by the presence of metal ions such as Zn^{2+} and Cu^{2+}, while the dissociation of [Gd(Medodpa)]$^+$ and [Gd(dodpa)]$^+$ is not affected by these metal ions.[8] These results imply that the substitution of the 1,7-diaza-12-crown-4 moiety of bp12c4^{2-} by a cyclen unit has a relatively small impact on the thermodynamic stability of the Gd^{3+} complexes (see above), while it has a beneficial effect on their kinetic inertness.
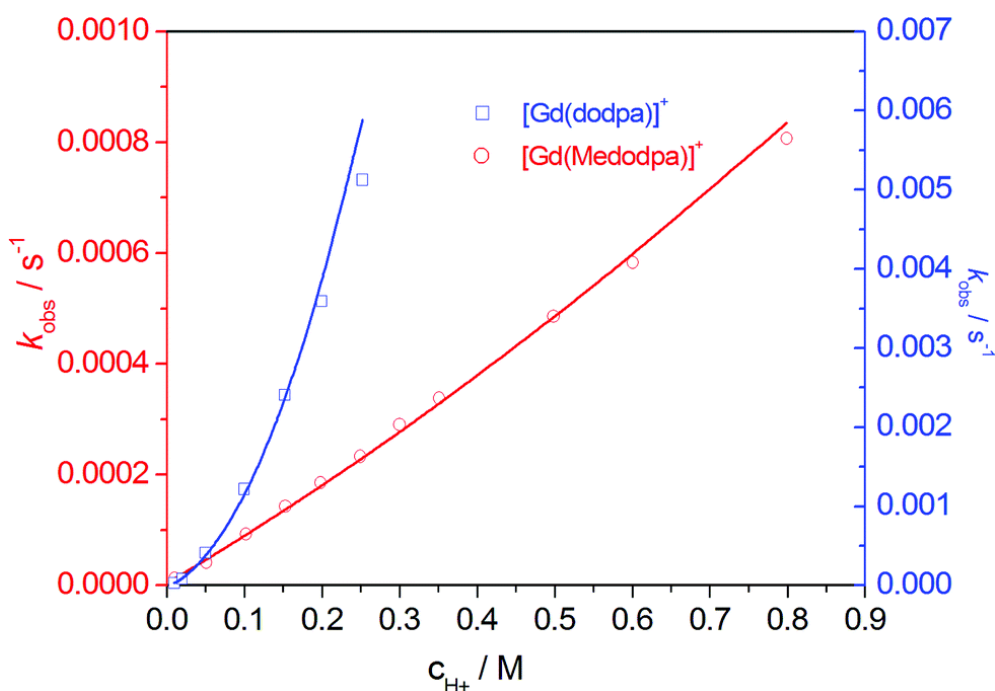
Fig. 5. Pseudo-first-order rate constants measured for the acid-assisted dissociation of $[Gd(dodpa)]^+$ and $[Gd(Medodpa)]^+$ complexes, k_{obs}, as a function of proton concentration. The solid lines correspond to the fits of the data as described in the text.

Mn^{2+} complexes are known to form kinetically less inert complexes than the Ln^{3+} ions, and thus their inertness can be easily accessed by following the transmetallation reactions occurring between the Mn^{2+} complexes and a suitable exchanging metal ion. The Cu^{2+} ion is usually selected for such a purpose as it allows using UV-vis spectrophotometry to gain the kinetic data. The metal exchange reactions of the [Mn(dodpa)] and [Mn(Medodpa)] complexes were studied in the presence of a high excess (10–40 fold) of the exchanging metal ion to ensure the pseudo-first-order conditions. Because the rates of the exchange reactions were found to be independent of the metal ion concentration, the direct involvement of the metal ion in the exchange process can be ruled out (in the pH range studied). This is somewhat surprising considering that the ligands offer eight potential donor atoms, while the coordination numbers observed more often in the literature for the Mn^{2+} ion are 6 and 7. However, this is consistent with the thermodynamic stability constants, which suggest the coordination of both picolinate pendant arms to the Mn^{2+} ion in the complexes, as for the complexes with uncoordinated donor atoms (*e.g.* $dota^{4-}$) the presence of an exchanging metal ion usually affects the dissociation rates.[31]

The rate constants k_{obs} plotted as a function of pH (Fig. 6) indicate a saturation like behaviour that turns into a nearly straight line for [Mn(dodpa)] at high $c_H{}^+$ concentration. The pseudo-first order rate constants determined were fitted to eqn (7) to give the rate constants presented in Table 3. The kinetic data indicate that the Mn^{2+} complexes of these dipicolinate ligands dissociate *via* the spontaneous and acid catalysed dissociation pathway, characterized by the k_0 and k_1 rate constants, respectively. In spite of the fact that the rate constants were evaluated using a wide pH range by including pH values up to pH = 4, the rate constants of spontaneous dissociation could not be determined with high accuracy (as the values determined were comparable to their uncertainties $k_0 = (2.2 \pm 2.9) \times 10^{-5}$ s^{-1} for [Mn(dodpa)] and $k_0 = (1.9 \pm 1.7) \times 10^{-5}$ s^{-1} for [Mn(Medodpa)]), so that the values reported here can be taken as the upper limits for these rate constants. Nevertheless, we decided to use them in the calculation of half-lives of the complexes, as near physiological conditions spontaneous dissociation represents the most important dissociation pathway. Besides this, for the [Mn(dodpa)] complex it was not possible to determine the second protonation constant ($K_{[M(H2)}L]$)) and the rate constant characterizing its dissociation through the diprotonated intermediate ($k^H{}_H$) independently, and

thus only their product (k_2 M^{-2} s^{-1}) was calculated and included in Table 3. This intermediate was not observed for the [Mn(Medodpa)] complex, which was found to be less inert than the complex of the unsubstituted dodpa^{2-} ligand, in contrast with the behaviour of the corresponding Gd^{3+} complexes. These results suggest that the steric hindrance brought by the methyl substituents affects negatively the kinetic inertness of the complexes formed with small metal ions such as Mn^{2+}.

Table 2. Proton dissociation rate constants of [Gd(dodpa)]$^+$ and [Gd(Medodpa)]$^+$ complexes and dissociation rates and half-lives calculated for [H]$^+$ = 0.1 M. Data for related systems are provided for comparison.

	dodpa^{2-}	Medodpa^{2-}	do3a^{3-} [a,b]	dota^{4-} [a,c]
k_0/s^{-1}		$3.8(9) \times 10^{-6}$		6.7×10^{-11}
$k_1/M^{-1} s^{-1}$	$2.5(4) \times 10^{-3}$	$8.3(4) \times 10^{-4}$	2.3×10^{-2}	1.8×10^{-6}
$k_2/M^{-2} s^{-1}$	$8.2(7) \times 10^{-2}$	$2.6(9) \times 10^{-4}$		
k_{obs}/s^{-1} at [H$^+$] = 0.1 M	1.08×10^{-3}	8.94×10^{-5}	2.3×10^{-3}	1.8×10^{-7}
$t_{1/2}/s$	641	7751	301	3.85×10^6

a From ref. 17. *b* Similar data were published by K. Kumar *et al.*, ref. 29. *c* Similar values were reported by Desreux *et al.*, ref. 30.
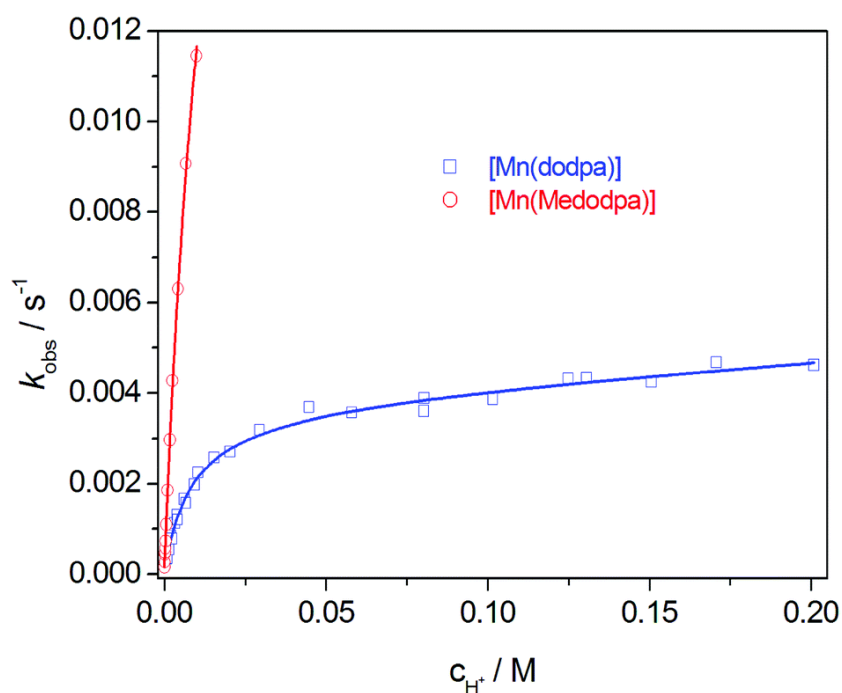

Fig. 6. Pseudo-first-order rate constants measured for the acid-assisted dissociation of [Mn(dodpa)] and [Mn(Medodpa)] complexes, k_{obs}, as a function of proton concentration. The solid lines represent the fits of the data to eqn (7).

Table 3. Equilibrium constants, rate constants and half-lives of the reactions characterising the dissociation of Mn^{2+} complexes (25 °C, $I = 0.15$ M NaCl, 0.1 M chloroacetic acid and 0.05 M dmp buffer).

	k_0/s^{-1}	k_1/M^{-1}s^{-1}	k_2/M^{-2}s^{-1}	k_3/M^{-1}s^{-1}	Log K_1^H	K_M ^{e}	$t_{1/2}$ ^{e}(h)
dodpa^{2-}	$(2.2 \pm 2.9) \times 10^{-5}$	0.46^b	0.61 ± 0.24		3.45(4)		8.90
Medodpa^{2-}	$(1.9 \pm 1.7) \times 10^{-5}$	97^c			3.01(1)		8.38
dompa^{-} ^{a}	1.2×10^{-3}	235			4.02		0.160
dota^{4-} ^{d}	1.8×10^{-7}	4.0×10^{-2}	1.6×10^3	1.5×10^{-5}	4.26	68	1037

a Taken from ref. 18. b The value represents the product of $k_H \times K_{[M(HL)]}$ where $k_H = (3.8 \pm 0.2) \times 0^{-3}$ s^{-1} and $K_{[M(HL)]} = 119 \pm 13$. c The value represents the product of $k_H \times K_{[M(HL)]}$ where $k_H = (1.8 \pm 0.1)$ s^{-1} and $K_{[M(HL)]} = 53 \pm 15$. d Taken from ref. 31. e pH = 7.4; the concentration of the Zn^{2+} exchanging metal ion used in the calculations was 1×10^{-5} M.

Self-aggregation of [La(dodpa)]$^+$

Slow evaporation of aqueous solutions of [La(dodpa)]$^+$ provided single crystals for X-ray diffraction measurements. Unfortunately, the poor quality of the crystals did not allow obtaining accurate structural data. However, the crystallographic data pointed to the presence of [La$_3$(dodpa)$_3$(H$_2$O)$_3$]$^{3+}$ trinuclear entities in the solid state formed by the presence of bridging carboxylate units. In a recent study we demonstrated that binucleating do3a^{3-} ligands containing different spacers undergo self-aggregation into nanoparticles, which was attributed to the presence of bridging carboxylate units.[32] In the light of these results, we decided to investigate whether the [La(dodpa)]$^+$ complex experiences self-aggregation in aqueous solutions. Thus, we have performed DOSY (diffusion-ordered NMR spectroscopy) experiments on D$_2$O solutions of the diamagnetic [La(dodpa)]$^+$ and [Lu(dodpa)]$^+$ complexes. Taking the diffusion coefficient of HDO as a reference ($D = 1.92 \times 10^{-10}$ m^2 s^{-1} at 298 K),[33] these experiments (Fig. 7) provided diffusion coefficients D at 298 K amounting to 2.51×10^{-10} and 3.78×10^{-10} m^2 s^{-1} for the La^{3+} and Lu^{3+} complexes, respectively. These data imply that the Lu^{3+} complex diffuses faster in solution than the La^{3+} complex, in line with the formation of aggregates in the latter case. These self-diffusion coefficients depend on the solution viscosity η, the van der Waals radius of the complex a, and a translational microviscosity factor f_S^t that accounts for the discrete nature of the solution through the Stokes–Einstein for translation (eqn (8)):[34]

$$D = \frac{k_B T}{6\pi a \eta} \tag{8}$$

This equation gives van der Waals radii of 4.69 and 7.07 Å for the Lu^{3+} and La^{3+} complexes at 298 K using the diffusion coefficients obtained from DOSY experiments and η(D$_2$O) $= 1.232 \times 10^{-3}$ Pa s.[35] DFT calculations performed on the [Lu(dodpa)]$^+$ complex using the TPSSh functional allowed us to estimate the volume of this complex, defined as the volume inside a contour of 0.001 electron Bohr^{-3}. We obtained a molecular volume of 501.89 Å^3, which is very similar to that reported for mononuclear complexes with a similar size.[36] The radius of the complex was then evaluated to be $a = 4.93$ Å by considering a sphere having the same volume. This value is in very good agreement with that obtained from DOSY measurements, indicating that the [Lu(dodpa)]$^+$ complex is present as a mononuclear species in solution.

The crystallographic data obtained for [La(dodpa)]$^+$ were used as an input geometry for structure optimization of [La$_3$(dodpa)$_3$(H$_2$O)$_3$]$^{3+}$. Due to the large size of this system, geometry optimizations were performed at the HF level (see the computational details below). Subsequent single point energy calculations using the TPSSh functional gave a molecular volume of 1663.77 Å^3, which corresponds to a sphere with a

radius of 7.35 Å. This value is in excellent agreement with that obtained from DOSY experiments (7.07 Å), which confirms that the La^{3+} complex of dodpa^{2-} forms stable trinuclear aggregates in aqueous solution. The optimized geometry of $[La_3(dodpa)_3(H_2O)_3]^{3+}$ (Fig. 8) shows that the trinuclear entity is stabilized by bridging bidentate carboxylate groups ($\mu_{1,3}$-carboxylate).[37] Hydrogen-bonding interactions involving the ligand NH groups and oxygen atoms of carboxylate groups of neighbouring $[La(dodpa)(H_2O)]^+$ units appear to provide additional stabilization to the trinuclear edifice. The four five-membered chelate rings formed upon coordination of the cyclen moiety adopt mixed ($\delta\lambda\delta\lambda$) conformations.[38]
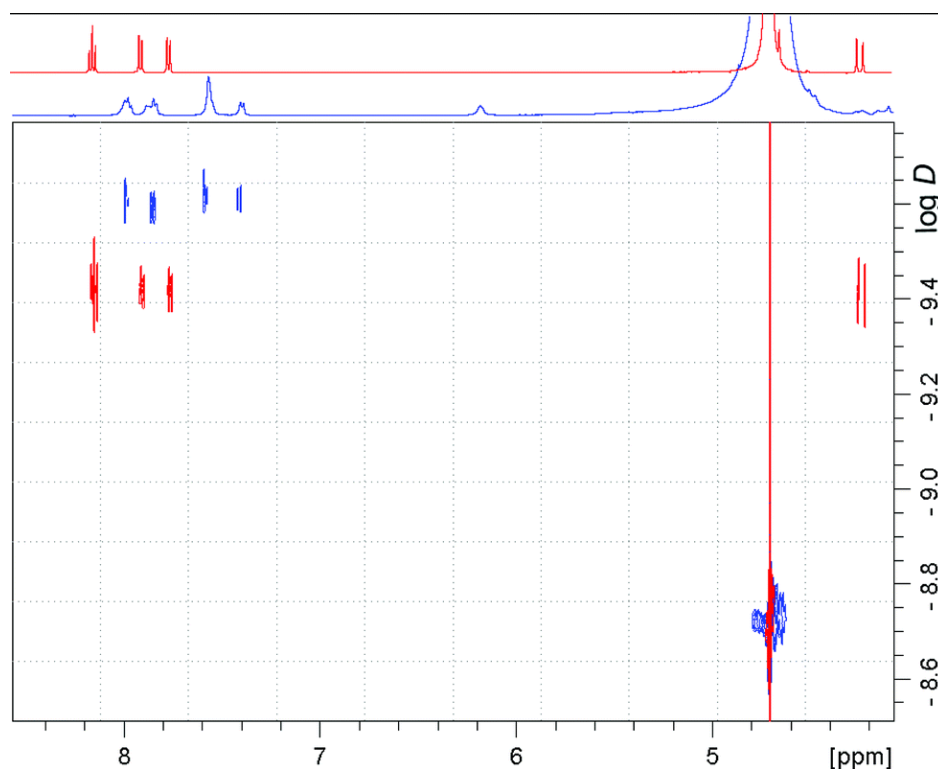

Fig. 7. Superposed ^{1}H DOSY (D$_2$O, 500 MHz, 298 K, pD ~ 7.0) experiments of $[Lu(dodpa)]^+$ (red) and $[La_3(dodpa)_3(H_2O)_3]^{3+}$(blue).

Further support for the formation of trinuclear edifices was provided by the ^{1}H NMR spectra and ESI-MS. Indeed, while the ^{1}H spectrum recorded for the $[Lu(dodpa)]^+$ complex is in agreement with an effective C_2 symmetry of the complex in solution, the spectrum of the La^{3+} analogue points to a C_1 symmetry (Fig. 7, see also Fig. S11, ESI†). The ^{1}H spectrum of the La^{3+} complex shows six signals due to proton nuclei of the pyridyl units, which indicates that the two picolinate pendant arms are magnetically non-equivalent. One of these signals is observed at a particularly high field (6.27 ppm). Inspection of the structure of the trimer obtained with HF calculations shows that a proton of one of the picolinate pendant arms is directed toward the aromatic ring current of a picolinate group of a neighbouring pendant arm (CH···C distances = 3.2–3.6 Å). The large low-frequency shift of the resonance due to this proton is therefore attributable to a ring current shift effect provoked by the neighbouring pyridyl unit, which results in a shielding for any nuclei above or below that ring. The ESI$^+$-MS of $[La(dodpa)]^+$ presents a peak at m/z 886.16 corresponding to the trinuclear entity $[(La(dodpa))_3Cl]^{2+}$, together with a peak at m/z 1193.21 due to $[(La(dodpa))_2Cl]^+$ and the peak due to the mononuclear complex $[La(dodpa)]^+$ at m/z 579.12 (Fig. S12, ESI†). The presence of peaks in the MS due to the monomeric (100%), trimeric (60%) and dimeric (2%) entities indicates dissociation of the aggregates under the mild conditions of the electrospray ionization, pointing to a relatively low stability of the trimer.
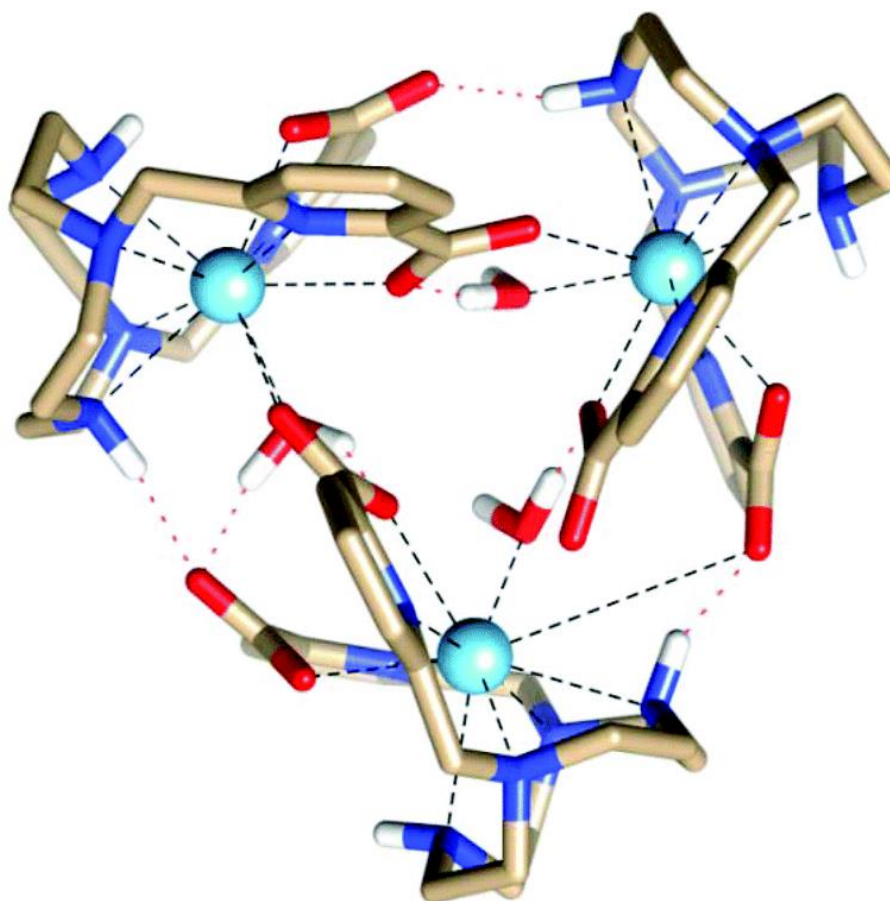
Fig. 8. Optimized geometry of $[La_3(dodpa)_3(H_2O)_3]^{3+}$ obtained with HF calculations. Hydrogen atoms attached to carbon atoms are omitted for simplicity.

X-ray structure of [Cu(dodpa)]·5H$_2$O

Single crystals of formula [Cu(Medodpa)]·5H$_2$O were obtained by slow evaporation of a concentrated aqueous solution of the complex, prepared by refluxing a 1 : 1 mixture of the ligand and copper(II) perchlorate at neutral pH (pH was adjusted by addition of K$_2$CO$_3$). Crystals contain the neutral complex [Cu(dodpa)] and water molecules establishing a hydrogen-bonding network with oxygen atoms of the carboxylate groups. A view of the structure of the complex is shown in Fig. 9, which also provides bond distances of the metal coordination environment. The metal ion is six-coordinated, being directly bound to four nitrogen donor atoms of the cyclen unit and the two donor atoms of one of the picolinate pendant arms. The second picolinate group remains uncoordinated. The distance from the metal ion and N1 is considerably longer than the remaining bond distances of the metal coordination environment [Cu1–N1 = 2.423(4) Å], which shows that this donor atom is weakly bound to the metal ion. A similar situation was previously observed for the [Cu(dompa)]$^+$ complex.[38]

Surprisingly, the cyclen unit adopts a conformation in which the five-membered chelate ring formed upon coordination of the ethylenediamine moieties of the ligand adopt a mixed conformation (λδλδ) instead of the (δδδδ) [or (λλλλ)] conformations often observed in the solid state for metal complexes with cyclen-based ligands (*i.e.* [Cu(dompa)]$^+$).[39] The coordination polyhedron can be best described as a distorted octahedron, with the *trans* angles O1–Cu1–N1 (151.57(11)°) and N4–Cu1–N2 (148.80(16)°) deviating considerably from the value expected for a regular octahedron (180°), and the *cis* angles falling within the range 74.7–116.2°.
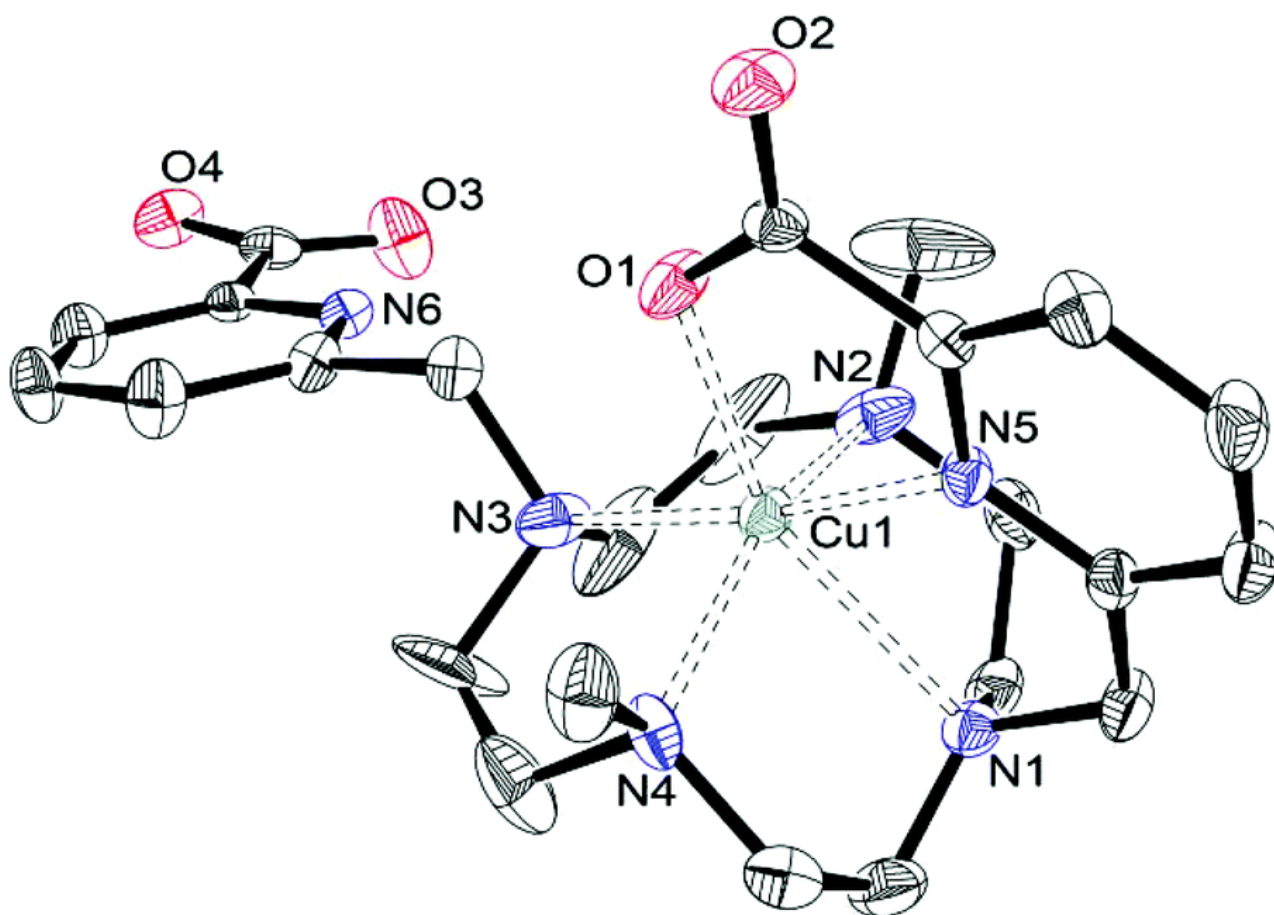
Fig. 9. View of the X-ray structure of the [Cu(Medodpa)] complex. The ORTEP plot is at the 30% probability level. Hydrogen atoms and water molecules are omitted for simplicity. Bond distances: Cu1–N1 2.423(4), Cu1–N2 2.135(5), Cu1–N3 2.062(5), Cu1–N4 2.102(5), Cu1–N5 2.045(4), Cu1–O1 2.201(4) Å.

Conclusions

We have herein reported the results of the equilibrium, dissociation kinetics, DFT and X-ray crystallographic studies performed for two cyclen derivatives featuring two picolinate moieties in *trans* positions to each other (1,7-disubstituted tetraazacyclododecane). The protonation constants of the ligands and thermodynamic stability constants of the complexes of dodpa^{2-} and Medodpa^{2-} formed with Mn^{2+}, Cu^{2+} and Gd^{3+} have been determined by a simultaneous fit of the data obtained by multiple methods (pH potentiometry, UV-vis spectrophotometry and ^{1}H-relaxometry). The stability constants of the complexes formed with dodpa^{2-} and Medodpa^{2-} do not differ significantly (*e.g.* log $K_{[Mn(dodpa)]}$ = 17.40 *vs.* log $K_{[Mn(Medodpa)]}$ = 17.46, log $K_{[Cu(dodpa)]}$ = 24.34–25.17 *vs.* log $K_{[Cu(Medodpa)]}$ = 24.74 and log $K_{[Gd(dodpa)]}^+$ = 17.27 *vs.* log $K_{[Gd(Medodpa)]}^+$ = 17.59), which indicates that the steric hindrance brought by the methyl groups has no significant effect on the stability of the complexes. Besides, the results reported indicate that these ligands form complexes with thermodynamic stability quite similar to that of the 1,7-dioxa-4,10-diazacyclododecane based bp12c4^{2-} chelator reported some years ago (the stability constants are about an order of magnitude lower than the value reported for [Gd(bp12c4)]$^+$ in the literature). At the same time the kinetic inertness of the Gd^{3+} complexes of dodpa^{2-} and Medodpa^{2-} is considerably higher than that of the [Gd(bp12c4)]$^+$ as evidenced by the noticeable decrease in the rate constant characterizing the acid catalyzed dissociation. This is very likely the consequence of the somewhat more compact and more rigid structure of the complexes of dodpa^{2-} and Medodpa^{2-} in comparison with the Gd^{3+} complex formed with the bp12c4^{2-} chelator. The considerable increase in the stability constants (*ca.* 3 log K units) and inertness of the [Mn(dodpa)] and [Mn(Medodpa)] complexes (characterized

by the calculated half-lives of the dissociation at pH = 7.4) *vs.* the corresponding data published for the cyclen monopicolinate derivative ([Mn(dompa)]$^+$) suggest that both picolinate moieties are involved in the coordination of Mn^{2+} in the dipicolinate derivatives. However, the stability of the Cu^{2+} complexes as well as the X-ray structure of the [Cu(Medodpa)] complex indicate that the ligand binds the Cu^{2+} ion in a hexadentate fashion, one of the picolinate arms remaining uncoordinated. The greater size of the lighter Ln^{3+} ions (*e.g.* La^{3+}), and the fact that the carboxylate moiety may bind the metal ions in a bridging mode, results in the formation of trinuclear complexes in solution. The existence of these species for the lighter and their absence for the heavier lanthanide ions was proved on diamagnetic [La(dodpa)]$^+$ and [Lu(dodpa)]$^+$ by means of NMR spectroscopy (DOSY) and DFT calculations.

Experimental and computational methods

General

ESI-TOF mass spectra were recorded using an LC-Q-q-TOF Applied Biosystems QSTAR Elite spectrometer in the positive ion mode. ^{1}H and ^{13}C NMR spectra were recorded on a Bruker Avance 500 spectrometer equipped with a dual cryoprobe or on a Bruker Avance 300 spectrometer. Chemical shifts are reported in δ values. The MnCl$_2$, CuCl$_2$ and GdCl$_3$ stock solutions were prepared from the chemicals of highest analytical grade using bidistilled water. The concentrations of the stock solutions were determined by complexometric titration with standardized Na$_2$H$_2$edta and eriochrome black T indicator in the presence of ascorbic acid and potassium hydrogen tartrate at pH = 10.0 (NH$_4$Cl/NH$_3$·H$_2$O buffer) for MnCl$_2$, murexide indicator at pH = 5.0 (urotropin buffer) for CuCl$_2$ and xylenol orange indicator at pH = 5.8 (urotropin buffer) for the GdCl$_3$ stock solution.

pH-Potentiometry

The protonation constants of the ligands (dodpa^{2-}, Medodpa^{2-} and do3a^{3-} for comparative purposes) and the equilibrium involving the Mn^{2+} and Cu^{2+} metal ions were studied by pH-potentiometry. The pH-potentiometric titrations were carried out with a Metrohm 785 DMP Titrino titration workstation with the use of a Metrohm 6.0233.100 combined electrode in the pH range of 1.8–11.8. For the calibration of the pH-meter, KH-phthalate (pH = 4.005) and borax (pH = 9.177) buffers were used, while the liquid junction potential was corrected by applying the method proposed by Irving *et al.*[40] A 0.15 M NaCl ionic strength was set in the samples and a CO$_2$-free NaOH stock solution (standardized by KH-phthalate titration) kept under a nitrogen protecting atmosphere was used as the titrant (c = 0.1914 M). The titrated samples (starting volume of 6 mL) were stirred mechanically and thermostated at 25.0 ± 0.1 °C using a circulating water bath. To avoid the effect of CO$_2$, N$_2$ gas was bubbled through them during the titration process. The protonation constants of the ligands were determined from the titration data obtained by titrating 1.94 and 2.73 mM (dodpa^{2-}), 2.56 and 2.86 mM (Medodpa^{2-}) and 1.86 mM (do3a^{3-}) ligand solutions with the base. The total number of fitted data was 384, 419 and 181 data pairs with fitting parameters (ΔV, defined as the difference between the experimental and calculated titration curves expressed in cm^3 of the titrant or as the difference between the experimental and calculated absorbances) of 2.93 × 10^{-3}, 3.27 × 10^{-3} and 5.86 × 10^{-3} cm^3, respectively). The concentrations of the ligand stock solutions were also determined from these data by comparing the titration curves obtained in the presence and absence of a 2-fold excess of Mn^{2+}. The stability constants of the Mn^{2+} complexes (two parallel titrations using 1.99, 2.94 mM and 2.54 mM solutions) solutions giving 376, 442 and 264 data pairs with fitting parameters ΔV = 3.79 × 10^{-3}, 4.98 × 10^{-3} and 6.15 × 10^{-3} cm^3 for the dodpa^{2-}, Medodpa^{2-} and do3a^{3-} ligands, respectively) and the protonation equilibria of the Cu^{2+} complexes were also studied by direct pH-potentiometry (two parallel titrations using 1.98 and 2.04 mM solutions providing 244 and 690 data pairs with ΔV = 5.59 and 4.33 × 10^{-3} cm^3), allowing five minutes for

the sample equilibrium to be attained. For the calculation of the equilibrium constants the PSEQUAD program was used.[41]

UV-vis spectrophotometry

The stability constants of the Cu^{2+} complexes (using the so-called batch method), as well as the metal exchange reactions of the Mn^{2+} complexes using the Cu^{2+} ion as a ligand scavenger, were studied by UV-vis spectrophotometry. The spectrophotometric measurements were performed with the use of a Cary 1E spectrophotometer at 25 ± 0.1 °C, using semi-micro 1.0 cm cuvettes. The molar absorptivities of $CuCl_2$ and the [Cu(dodpa)], [Cu(Hdodpa)]$^+$, [Cu(Medodpa)] and [Cu(HMedodpa)]$^+$ complexes were determined at 21 wavelengths (550–750 nm range) by recording the spectra of 2.0×10^{-3}, 4.0×10^{-3}, 6.0×10^{-3} and 8.0×10^{-3} M solutions. The molar absorptivities of the [Cu(H$_2$dodpa)]$^{2+}$ complex at the same wavelengths were determined by fitting the pH-potentiometric and UV-vis spectrophotometric data simultaneously when the molar absorptivity of the species present in the equilibrium was known (and fixed) from independent experiments. The stability of the Cu^{2+} complexes was also determined by competition titration with the use of the open chain ligand derivative bis(aminomethyl)phosphinic acid (bimp^{5-}). The equilibrium in the Cu^{2+}-bimp^{5-}-H$^+$ system has been studied previously in the literature[24] by multiple methods, but it was also determined in the current study from the simultaneous fit of the pH-potentiometric and UV-vis spectrophotometric (batch samples) titration results. The protonation and stability constants determined are as follows: $\log \beta_{[HL]} = 9.36(1)$, $\log \beta_{[H2L]} = 15.92(1)$, $\log \beta_{[H3L]} = 18.69(2)$, $\log \beta_{[H4L]} = 20.74(2)$, $\log \beta_{[H5L]} = 22.23(5)$, $\log \beta_{[CuL]} = 18.39(3)$ and $\log \beta_{[CuHL]} = 21.19(2)$ with a fitting parameter of 4.99×10^{-3} cm^3 for the 219 data pairs fitted. The competition titrations were carried out in the pH ranges of 3.6–4.0 (dodpa^{2-}) and 3.6–4.3 (Medodpa^{2-}) where the exchange reaction was found to occur within 24 hours. Samples containing 1.99 mM Cu^{2+} and 2.042 mM dodpa^{2-} or 1.99 mM Cu^{2+} and 2.019 mM Medodpa^{2-} with increasing amounts of the bimp^{5-} ligand (in the concentration range 2.052–50.05 mM for dodpa^{2-} and 2.002–80.28 mM for Medodpa^{2-}) were prepared, equilibrated and visible spectra recorded. Being in possession of the molar absorption coefficients of all the absorbing species the cumulative constants characterizing the formation of the [Cu(HL)]$^+$ (L = dodpa^{2-} and Medodpa^{2-} ligands) complexes were estimated.

The decomplexation reactions of the Mn^{2+} complexes were carried out using the Cu^{2+} ion as the exchanging metal ion in the pH ranges $0.77 - 3.05$ and $2.00 - 4.09$ for the dodpa^{2-} and Medodpa^{2-} complexes, respectively. The concentration of the complexes was set to 2.5×10^{-4} M, while the exchange reactions were performed under pseudo-first order conditions where the metal ion was in a 20 fold excess (the direct involvement of the metal ion in the dissociation reaction was ruled out by studying the effect of 10–40 fold metal ion excess with the samples of relatively high pH) at 310 nm. The kinetic studies were carried out using chloroacetic acid ($\log K^H{}_1 = 2.85$) and N,N'-dimethyl-piperazine (dmp, $\log K^2{}_H = 4.19$) buffers at 0.10 M and 0.05 M concentrations to maintain constant the pH in the samples. The pseudo-first-order rate constants (k_{obs}) were calculated by fitting the absorbance–time data pairs to the following equation:

$$X_t = (X_0 - X_e)e^{-k_{obs}t} + X_e \tag{9}$$

where X_t, X_0 and X_e are the absorbance (or relaxivity) at time t, at the start and at equilibrium, respectively. The calculations were performed with the computer program Micromath Scientist, version 2.0 (Salt Lake City, UT, USA), using a standard least-squares procedure.

¹H-relaxometry

The relaxivity, the stability constants of the Mn^{2+} and Gd^{3+} complexes and kinetic inertness of the Gd^{3+} complexes were studied using ¹H-relaxometry. The longitudinal relaxation times (T_1) of water protons were measured at 20 MHz with a Bruker Minispec MQ-20 NMR analyzer at 25.0 ± 0.2 °C (set and controlled with the use of a circulating water bath). T_1 values were measured using the inversion recovery method ($180°–\tau–90°$) by averaging 5–6 data points obtained at 14 different τ values (measurements on the equilibrated samples) while single T_1 values obtained at 8 different τ values were collected and fitted as a function of time in the kinetic measurements. The relaxivities ($mM^{-1}\ s^{-1}$) of the complexes were determined using standard methodology (by plotting the reciprocal longitudinal relaxation times of the complexes against their concentrations). Owing to the slow complex formation, the stability of the Gd^{3+} complexes was determined by promoting the partial to full dissociation of the complexes in batch samples (1 mM) covering the pH range 2.5–8.0 set with the use of a buffer cocktail consisting of 25 : 25 : 25 mM of piperazine (pip), N-methyl-piperazine (nmp) and N,N'-dimethyl-piperazine (dmp). In order to determine the time needed for equilibration (4 months), three representative samples with pH = 3.00, 4.94 and 7.05 were prepared and their relaxivities recorded as a function of time. The relaxivities of the batch samples were repeatedly measured one year later in order to confirm that the equilibrium was indeed attained. The equilibrium involving the Mn^{2+} ion was considerably faster as relaxivities of the batch samples prepared by mixing equimolar amounts of Mn^{2+} and dodpa^{2-} or Medodpa^{2-} ligands (2.5–2.5 mM each) and various amounts of acid (covering the pH range of 1.93–6.67 and 1.90–3.51 for the dodpa^{2-} or Medodpa^{2-} systems, respectively) became constant within 5 minutes from their preparation. The kinetic inertness of the [Gd(dodpa)]$^+$ and [Gd(Medodpa)]$^+$complexes was characterized by studying the acid catalyzed dissociation of the complexes under pseudo first order conditions (1 mM Gd^{3+} complex solutions were studied in the acid concentration range of 9.87–25.2 mM and 10.1–79.9 mM, respectively). The kinetic profiles obtained by recording the relaxivity as a function of time were fitted to eqn (9) using the Scientist™ program. In these calculations the relaxivities of the complex and the Gd^{3+} ion (at 25 °C and 20 MHz) were fixed to their values determined independently.

X-ray crystallography

X-ray diffraction data of [Cu(Medodpa)]·5H$_2$O (**1**) were collected with a circular diffractometer X-Calibur-2 CCD 4 (Oxford Diffraction), including a four circle goniometer (KM4) and a two dimensional CCD detector (SAPPHIRE 2). Three dimensional X-ray diffraction data were collected on an X-CALIBUR-2 CCD 4-circle diffractometer (Oxford Diffraction). Data reduction, including inter-frame scaling, Lorentz, polarization, empirical absorption and detector sensitivity corrections, was carried out using attached programs of Crysalis software[42] (Oxford Diffraction). Complex scattering factors were taken from the program SHELX97[43] running under the WinGX program system.[44] The structure was solved by direct methods with SIR-97[45] and refined by full-matrix least-squares on F^2. X-ray diffraction data of Na[H$_4$Medodpa](CF$_3$COO)$_3$·CF$_3$COOH (**2**) were collected on a Bruker Kappa APEXII CCD diffractometer. Data were corrected for Lorentz and polarization effects and for absorption by semiempirical methods[46] based on symmetry-equivalent reflections. Complex scattering factors were taken from the program SHELX97[43]running under the WinGX program system[44] as implemented on a Pentium® computer. The structure was solved by direct methods using SHELXS97[43] and refined[43] by full-matrix least-squares on F^2. All hydrogen atoms were included in calculated positions and refined in riding mode, except those of the disordered CF$_3$COOH molecule present in crystals of **2**, which were located in a difference electron-density map and the torsion angle refined. Crystal data and details of data collection and refinement are summarized in Table 4. CCDC 1017211 and 1015477 contain the supplementary crystallographic data for this paper.

Table 4. Crystal data and refinement details of [Cu(Medodpa)]·5H$_2$O (**1**) and
Na[H$_4$Medodpa](CF$_3$COO)$_3$·CF$_3$COOH (**2**).

	1	**2**
Formula	C$_{24}$H$_{42}$CuN$_6$O$_9$	C$_{32}$H$_{37}$F$_{12}$N$_6$NaO$_{12}$
MW	622.18	948.66
Crystal system	Orthorhombic	Monoclinic
Space group	$P2_12_12_1$	$P2_1/c$
T/K	300(2)	100(2)
a/Å	10.2042(7)	20.412(2)
b/Å	16.8211(11)	9.4077(10)
c/Å	16.8403(11)	21.531(3)
α/°	90	90
β/°	90	101.241(6)
γ/°	90	90
V/Å^3	2890.6(3)	4055.3(8)
F(000)	1316	1944
Z	4	4
λ/Å(MoK$_\alpha$)	0.71073	0.71073
D_{calc}/g cm^{-3}	1.43	1.554
μ/mm^{-1}	0.815	0.161
θ Range/°	3.14 to 26.37	1.929 to 26.372
R_{int}	0.0952	0.0877
Reflns measd	22 452	45 414
Unique reflns	5901	8301
Reflns obsd	3242	6136
GOF on F^2	0.817	1.036
R_1 ^{a}	0.0516	0.0626
wR_2 (all data)^b	0.0907	0.1827
Largest differences peak and hole/e Å^{-3}	0.712/−0.319	0.794/−0.478

a $R_1 = \sum||F_o| - |F_c||/\sum|F_o|$. b w$R_2 = \{\sum[w(||F_o|^2 - |F_c|^2)^2]/\sum[w(F_o^4)]\}^{1/2}$.

Computational methods

All calculations were performed employing the Gaussian 09 package (revision B.01).[47] Full geometry optimizations of the [La$_3$(dodpa)$_3$(H$_2$O)$_3$]$^{3+}$ system were performed in the gas phase at the HF level by using the quasirelativistic effective core potential (ECP) of Dolg *et al.* and the related [5s4p3d]-GTO valence basis set for the lanthanides,[48] and the 3-21G basis set for C, H, N and O atoms. Although small, HF calculations employing this basis set in combination with the f-in-core ECP of Dolg were shown to provide molecular geometries of macrocyclic Ln^{3+} complexes in good agreement with the experimental structures observed by single-crystal X-ray diffraction studies.[49] No symmetry constraints have been imposed during the optimizations. Due to the considerable computational effort involving the calculation of second derivatives the optimized geometries were not characterized using frequency analysis. Full geometry optimizations of the [Lu(Medodpa)]$^+$ system were performed in aqueous solution employing DFT within the hybrid meta-GGA approximation with the TPSSh exchange–correlation functional,[50] in combination with the ECP of

Dolg *et al.*[48] for the lanthanide and the standard 6-31G(d) basis set for the ligand atoms. Solvent effects were included using the integral equation formalism of the polarizable continuum model (IEFPCM).[51] The stationary points found on the potential energy surfaces as a result of the geometry optimizations have been tested to represent energy minima rather than saddle points *via* frequency analysis. Molecular volumes, defined as the volume inside a contour of 0.001 electron Bohr^{-3}, were calculated at the TPSSh/6-31G(d) level using the volume = tight keyword in Gaussian 09.

Acknowledgments

References

1.   T. J. Wadas, E. H. Wong, G. R. Weisman and C. J. Anderson, *Chem. Rev.*, 2010, **110**, 2858; R. E. Mewis and S. J. Archibald, *Coord. Chem. Rev.*, 2010, **254**, 1686.

2.   P. Caravan, J. J. Ellison, T. J. McMurry and R. B. Lauffer, *Chem. Rev.*, 1999, **99**, 2293; *The Chemistry of Contrast Agents in Medical Magnetic Resonance Imaging*, ed. A. E. Merbach, L. Helm and É. Tóth, 2nd edn, Wiley, Chichester, 2013.

3.   J.-C. G. Bünzli, *Chem. Rev.*, 2010, **110**, 2729.

4.   E. Toth, E. Brucher, I. Lazar and I. Toth, *Inorg. Chem.*, 1994, **33**, 4070; C. A. Chang, L. C. Francesconi, M. F. Malley, K. Kumar, J. Z. Gougoutas, M. F. Tweedle, D. W. Lee and L. J. Wilson, *Inorg. Chem.*, 1993, **32**, 3501.

5.   U. Hennrich, L. Seyler, M. Schafer, U. Bauder-Wust, M. Eisenhut, W. Semmler and T. Bauerle, *Bioorg. Med. Chem.*, 2012, **20**, 1502; C. Chollet, R. Bergmann, J. Pietzsch and A. G. Beck-Sickinger, *Bioconjugate Chem.*, 2012, **23**, 771; J. Notni, J. Simecek, P. Hermann and H.-J. Wester, *Chem. – Eur. J.*, 2011, **17**, 14718; M. T. Ma, O. C. Neels, D. Denoyer, P. Roselt, J. A. Karas, D. B. Scanlon, J. M. White, R. J. Hicks and P. S. Donnelly, *Bioconjugate Chem.*, 2011, **22**, 2093.

6.   N. Chatterton, Y. Bretonniere, J. Pecaut and M. Mazzanti, *Angew. Chem., Int. Ed.*, 2005, **44**, 7595; L. Charbonnière, N. Weibel, C. Estournes, C. Leuvrey and R. Ziessel, *New J. Chem.*, 2004, **28**, 777.

7.   C. Platas-Iglesias, M. Mato-Iglesias, K. Djanashvili, R. N. Muller, L. Vander Elst, J. A. Peters, A. de Blas and T. Rodríguez-Blas, *Chem. – Eur. J.*, 2004, **10**, 3579; M. Mato-Iglesias, E. Balogh, C. Platas-Iglesias, É. Tóth, A. de Blas and T. Rodríguez-Blas, *Dalton Trans.*, 2006, 5404; A. Nonat, P. H. Fries, J. Pecaut and M. Mazzanti, *Chem. – Eur. J.*, 2007, **13**, 8489; N. Chatterton, C. Gateau, M. Mazzanti, J. Pecaut, A. Borel, L. Helm and A. E. Merbach, *Dalton Trans.*, 2005, 1129; S. Mameri, L. Charbonnière and R. Ziessel, *Tetrahedron Lett.*, 2007, **48**, 9132; A. Nonat, M. Giraud, C. Gateau, P. H. Fries, L.

Helm and M. Mazzanti, *Dalton Trans.*, 2009, 8033 ; E. W. Price, J. F. Cawthray, G. A. Bailey, C. L. Ferreira, E. Boros, M. J. Adam and C. Orvig, *J. Am. Chem. Soc.*, 2012, **134**, 8670; E. Boros, C. L. Ferreira, J. F. Cawthray, E. W. Price, B. O. Patrick, D. W. Wester, M. J. Adam and C. Orvig, *J. Am. Chem. Soc.*, 2010, **132**, 15726; E. Boros, J. F. Cawthray, C. L. Ferreira, B. O. Patrick, M. J. Adam and C. Orvig, *Inorg. Chem.*, 2012, **51**, 6279; G. A. Bailey, E. W. Price, B. M. Zeglis, C. L. Ferreira, E. Boros, M. J. Lacasse, B. O. Patrick, J. S. Lewis, M. J. Adam and C. Orvig, *Inorg. Chem.*, 2012, **51**, 12575; M. Roger, L. M. P. Lima, M. Frindel, C. Platas-Iglesias, J.-F. Gestin, R. Delgado, V. Patinec and R. Tripier, *Inorg. Chem.*, 2013, **52**, 5246; L. M. P. Lima, Z. Halime, R. Marion, N. Camus, R. Delgado, C. Platas-Iglesias and R. Tripier, *Inorg. Chem.*, 2014, **53**, 5269.

8. Z. Palinkas, A. Roca-Sabio, M. Mato-Iglesias, D. Esteban-Gomez, C. Platas-Iglesias, A. de Blas, T. Rodriguez-Blas and É. Toth, *Inorg. Chem.*, 2009, **48**, 8878.

9. M. Mato-Iglesias, A. Roca-Sabio, Z. Palinkas, D. Esteban-Gómez, C. Platas-Iglesias, E. Toth, A. de Blas and T. Rodriguez-Blas, *Inorg. Chem.*, 2008, **47**, 7840.

10. E. Balogh, M. Mato-Iglesias, C. Platas-Iglesias, É. Tóth, K. Djanashvili, J. A. Peters, A. de Blas and T. Rodríguez-Blas, *Inorg. Chem.*, 2006, **45**, 8719.

11. M. Regueiro-Figueroa, B. Bensenane, E. Ruscsák, D. Esteban-Gómez, L. J. Charbonnière, G. Tircsó, I. Tóth, A. de Blas, T. Rodríguez-Blas and C. Platas-Iglesias, *Inorg. Chem.*, 2011, **50**, 4125.

12. A. Roca-Sabio, M. Mato-Iglesias, D. Esteban-Gómez, É. Tóth, A. de Blas, C. Platas-Iglesias and T. Rodríguez-Blas, *J. Am. Chem. Soc.*, 2009, **131**, 3331; M. P. Jensen, R. Chiarizia, I. A. Shkrob, J. S. Ulicki, B. D. Spindler, D. J. Murphy, M. Hossain, A. Roca-Sabio, C. Platas-Iglesias, A. de Blas and T. Rodríguez-Blas, *Inorg. Chem.*, 2014, **53**, 6003.

13. M. Mato-Iglesias, C. Platas-Iglesias, K. Djanashvili, J. A. Peters, É. Tóth, E. Balogh, R. N. Muller, L. Vander Elst, A. de Blas and T. Rodríguez-Blas, *Chem. Commun.*, 2005, 4729.

14. C. Platas-Iglesias, C. Piguet, N. Andre and J.-C. G. Bunzli, *J. Chem. Soc., Dalton Trans.*, 2001, 3084; A. D'Aleo, A. Piccot, P. L. Baldeck, C. Andraud and O. Maury, *Inorg. Chem.*, 2008, **47**, 10269; A.-S. Chauvin, S. Gras and J.-C. G. Bünzli, *Org. Biomol. Chem.*, 2003, **1**, 737; R. Tripier, M. Hollenstein, M. Elhabiri, A.-S. Chauvin, G. Zucchi, C. Piguet and J.-C. G. Bunzli, *Helv. Chim. Acta*, 2002, **85**, 1915; A. Piccot, A. D'Aleo, P. L. Baldeck, A. Grichine, A. Duperray, C. Andraud and O. Maury, *J. Am. Chem. Soc.*, 2008, **130**, 1532; M.-L. Teyssot, L. Nauton, J.-L. Canet, F. Cisnetti, A. Chevry and A. Gautier, *Eur. J. Org. Chem.*, 2010, 3507; Z. E. A. Chamas, X. Guo, J.-L. Canet, A. Gautier, D. Boyer and R. Mahiou, *Dalton Trans.*, 2010, **39**, 7091.

15. A. Rodríguez-Rodríguez, D. Esteban-Gómez, A. de Blas, T. Rodríguez-Blas, M. Fekete, M. Botta, R. Tripier and C. Platas-Iglesias, *Inorg. Chem.*, 2012, **51**, 2509; A. Rodríguez-Rodríguez, D. Esteban-Gómez, A. de Blas, T. Rodríguez-Blas, M. Botta, R. Tripier and C. Platas-Iglesias, *Inorg. Chem.*, 2012, **51**, 13419.

16. B. Drahos, I. Lukes and É. Toth, *Eur. J. Inorg. Chem.*, 2012, 1975; G. A. Rolla, C. Platas-Iglesias, M. Botta, L. Tei and L. Helm, *Inorg. Chem.*, 2013, **52**, 3268; G. S. Loving, S. Mukherjee and P. Caravan, *J. Am. Chem. Soc.*, 2013, **135**, 4620.

17. A. Takács, R. Napolitano, M. Purgel, A. C. Bényei, L. Zékány, E. Brücher, I. Tóth, Z. Baranyai and S. Aime, *Inorg. Chem.*, 2014, **53**, 2858.

18. E. Molnar, N. Camus, V. Patinec, G. A. Rolla, M. Botta, G. Tircsó, F. K. Kálmán, T. Fodor, R. Tripier and C. Platas-Iglesias, *Inorg. Chem.*, 2014, **53**, 5136.

19. R. Ferreirós-Martínez, D. Esteban-Gómez, C. Platas-Iglesias, A. de Blas and T. Rodríguez-Blas, *Dalton Trans.*, 2008, 5754.

20. M. Woods, S. Aime, M. Botta, J. A. K. Howard, J. M. Moloney, M. Navet, D. Parker, M. Port and O. Rousseaux, *J. Am. Chem. Soc.*, 2000, **122**, 9781; S. Aime, A. Barge, J. I. Bruce, M. Botta, J. A. K. Howard, J. M. Moloney, D. Parker, A. S. De Sousa and M. Woods, *J. Am. Chem. Soc.*, 1999, **121**, 5762.

21. A. Bianchi, L. Calabi, C. Giorgi, P. Losi, P. Mariani, D. Palano, P. Paoli, P. Rossi and B. Valtancoli, *J. Chem. Soc., Dalton Trans.*, 2001, 917.

22. D. Eteban-Gómez, C. Cassino, M. Botta and C. Platas-Iglesias, *RSC Adv.*, 2014, **4**, 7094.

23. J. Xu, S. J. Franklin, D. W. Whisenhunt and K. N. Raymond, *J. Am. Chem. Soc.*, 1995, **117**, 7245.

24. N. Veronika Nagy, T. Szabó-Plánka, G. Tircsó, R. Király, Z. Árkosi, A. Rockenbauer and E. Brücher, *J. Inorg. Biochem.*, 2004, **98**, 1655.

25. H. D. Powell, O. M. Ni Dhubhghaill, D. Pubanz, L. Helm, Y. Lebedev, W. Schlaepfer and A. E. Merbach, *J. Am. Chem. Soc.*, 1996, **118**, 9333.

26. L. Sarka, L. Burai and L. E. Brucher, *Chem. – Eur. J.*, 2000, **6**, 719.

27. E. Brucher, G. Laurenczy and Z. Makra, *Inorg. Chim. Acta*, 1987, **139**, 141.

28. G. Tircsó, Z. Kovacs and A. D. Sherry, *Inorg. Chem.*, 2006, **45**, 9269.

29. K. Kumar and M. F. Tweedle, *Pure Appl. Chem.*, 1993, **65**, 515.

30. X. Y. Wang, T. Z. Jin, V. Comblin, A. Lopezmut, E. Merciny and J. F. Desreux, *Inorg. Chem.*, 1992, **31**, 1095.

31. B. Drahos, V. Kubicek, C. S. Bonnet, P. Hermann, I. Lukes and E. Toth, *Dalton Trans.*, 2011, **40**, 1945.

32. M. Regueiro-Figueroa, A. Nonat, G. A. Rolla, D. Esteban-Gomez, A. de Blas, T. Rodriguez-Blas, L. J. Charbonniere, M. Botta and C. Platas-Iglesias, *Chem. – Eur. J.*, 2013, **19**, 11696.

33. L. G. Longsworth, *J. Phys. Chem.*, 1960, **64**, 1914.

34. S. Rast and P. H. Fries, *J. Chem. Phys.*, 2000, **113**, 8724.

35. G. Jones and H. J. Fornwalt, *J. Chem. Phys.*, 1936, **4**, 30.

36. A. Roca-Sabio, C. S. Bonnet, M. Mato-Iglesias, D. Esteban-Gómez, É. Tóth, A. de Blas, T. Rodríguez-Blas and C. Platas-Iglesias, *Inorg. Chem.*, 2012, **51**, 10893.

37. M. A. Gil, W. Maringgele, S. Dechert and F. Meyer, *Z. Anorg. Allg. Chem.*, 2007, **633**, 2178.

38. L. M. P. Lima, D. Esteban-Gómez, R. Delgado, C. Platas-Iglesias and R. Tripier, *Inorg. Chem.*, 2012, **51**, 6916.

39. J. K. Beattie, *Acc. Chem. Res.*, 1971, **4**, 253.

40. H. M. Irving, M. G. Miles and L. D. Pettit, *Anal. Chim. Acta*, 1967, **38**, 475.

41. L. Zekany and I. Nagypál, *Computational Methods for the Determination of Formation Constants*, ed. D. J. Leggett, Plenum Press, New York, 1985, p. 291.

42. *Crysalis software system, version 1.171.28 cycle 4 beta*, Oxford Diffraction Ltd, Abingdon, U.K., 2005.

43. G. M. Sheldrick, SHELX, *Acta Crystallogr., Sect. A: Fundam. Crystallogr.*, 2008, **64**, 112.

44. L. J. Farrugia, WinGX MS-Windows system of programs for solving, refining and analysing single crystal X-ray diffraction data for small molecules, *J. Appl. Crystallogr.*, 1999, **32**, 837.

45. A. Altomare, M. C. Burla, M. Camalli, G. L. Cascarano, C. Giacovazzo, A. Guagliardi, A. G. G. Moliterni, G. Polidori and R. Spagna, SIR97, *J. Appl. Crystallogr.*, 1999, **32**, 115.

46. G. M. Sheldrick, *SADABS Version 2.10*, University of Göttingen, Germany, 2004.

47. M. J. Frisch, G. W. Trucks, H. B. Schlegel, G. E. Scuseria, M. A. Robb, J. R. Cheeseman, G. Scalmani, V. Barone, B. Mennucci, G. A. Petersson, H. Nakatsuji, M. Caricato, X. Li, H. P. Hratchian, A. F. Izmaylov, J. Bloino, G. Zheng, J. L. Sonnenberg, M. Hada, M. Ehara, K. Toyota, R. Fukuda, J. Hasegawa, M. Ishida, T. Nakajima, Y. Honda, O. Kitao, H. Nakai, T. Vreven, J. A. Montgomery Jr., J. E. Peralta, F. Ogliaro, M. Bearpark, J. J. Heyd, E. Brothers, K. N. Kudin, V. N. Staroverov, R. Kobayashi, J. Normand, K. Raghavachari, A. Rendell, J. C. Burant, S. S. Iyengar, J. Tomasi, M. Cossi, N. Rega, J. M. Millam, M. Klene, J. E. Knox, J. B. Cross, V. Bakken, C. Adamo, J. Jaramillo, R. Gomperts, R. E. Stratmann, O. Yazyev, A. J. Austin, R. Cammi, C. Pomelli, J. W. Ochterski, R. L. Martin, K. Morokuma, V. G. Zakrzewski, G. A. Voth, P. Salvador, J. J. Dannenberg, S. Dapprich, A. D. Daniels, Ö. Farkas, J. B. Foresman, J. V. Ortiz, J. Cioslowski and D. J. Fox, *Gaussian 09, Revision B.01*, Gaussian, Inc., Wallingford, CT, 2009.

48. M. Dolg, H. Stoll, A. Savin and H. Preuss, *Theor. Chim. Acta*, 1989, **75**, 173.

49. U. Cosentino, A. Villa, D. Pitea, G. Moro, V. Barone and A. Maiocchi, *J. Am. Chem. Soc.*, 2002, **124**, 4901.

50. J. M. Tao, J. P. Perdew, V. N. Staroverov and G. E. Scuseria, *Phys. Rev. Lett.*, 2003, **91**, 146401.

51. J. Tomasi, B. Mennucci and R. Cammi, *Chem. Rev.*, 2005, **105**, 2999.